Liquid Solid Mass Transfer in Small Diameter Trickle Bed Reactors

Lucille Naidoo

Liquid Solid Mass Transfer in Small Diameter Trickle Bed Reactors

Lucille Naidoo

Submitted in partial fulfilment of the requirements of the degree Masters in Engineering (Chemical Engineering) in the Faculty of Engineering, Built Environment and Information Technology, University of Pretoria, Pretoria.

9 July 2011

Liquid Solid Mass Transfer in Small Diameter Trickle Bed Reactors

Author: Lucille Naidoo

Supervisor: W. Nicol

Department: Department of Chemical Engineering
University of Pretoria

Degree: Master of Engineering (Chemical Engineering)

Synopsis

Trickle bed reactors form an integral component of the petrochemical industry. In order to optimise their performance, industrial reactors are scaled down to laboratory scale reactors. It is desired that the laboratory scale reactor ought to operate at the same superficial velocity to replicate the hydrodynamics of the industrial reactor. This can be achieved by scaling down reactors according to the reactor diameter. However, wall effects can severely impact the hydrodynamics of these small diameter laboratory scale reactors

The complex distribution of liquid in a trickle bed reactor operated in the trickle flow regime results in partial wetting of the solid particles which impacts the liquid solid mass transfer coefficient and consequently influences the reaction rates in a trickle bed reactor. The distribution of liquid in the trickle flow regime is also affected by prewetting procedures applied to the packed bed, where multiple hydrodynamic states occur. This phenomenon of hydrodynamic multiplicity affects the values of hydrodynamic parameters and complicates the prediction of trickle bed reactor performance.

In this study the liquid solid mass transfer was investigated in a variety of columns, with column to particle diameter ratios in the range of 10 to 1, by employing the electrochemical technique. A distinct trend was found where the decrease in column diameter resulted in an increase in the effective liquid solid mass transfer coefficient, even though the values of the effective liquid solid mass transfer coefficients were two orders of magnitude lower than published data. A threefold increase of the effective liquid solid mass transfer coefficient was obtained on decreasing the

column to particle diameter ratio from 10 to 3. However, this trend was not sustained for the bead column ($D/d_p=1$) where a decrease in effective liquid solid mass transfer coefficient was observed on decreasing the column to diameter ratio from 3 to 1. The substantial increase in liquid solid mass transfer could not be entirely explained by partial external wetting as well as interstitial velocity variations. The low values of liquid solid mass transfer coefficients also could not be explained despite attempts to validate the measurement technique.

The effects of hydrodynamic multiplicity on the effective liquid solid mass transfer coefficients were significant in all the columns. The Kan prewetting outperformed the Levec gas prewetting by as much as 1.5 times, while the super prewetting outperformed Levec prewetting by as much as 1.3 times. The modes without gas outperformed the modes with gas which is contrary to previous findings on the effect of gas on liquid solid mass transfer.

Keywords: Liquid solid mass transfer coefficient, wall effects, multiplicity, pre-wetting

Table of Contents

List of Tables

List of Figures

Nomenclature

a_s liquid solid mass transfer area per unit reactor volume (m^2/m^3)

a_c geometrical external packing area, external surface packing per unit reactor volume (m^2/m^3)

A_c cross-sectional area of column (m^2)

A_e area of wetted part of electrode (m^2)

A geometric area of electrode (m^2)

C concentration of electrolyte ($mol.m^{-3}$)

c_i concentration of the soluble material at the liquid solid interface ($kg\ mol.m^{-3}$)

c_o concentration of the soluble material in the outlet liquid ($kg\ mol.m^{-3}$)

D column diameter (m)

D_{iff} molecular diffusivity ($m^2.s^{-1}$)

D_i internal diffusivity ($m^2.s^{-1}$)

$(D_i)_{app}$ apparent internal diffusivity ($m^2.s^{-1}$)

d_p particle diameter (m)

F Faraday number ($C.mol^{-1}$) (equation 2)

F total flow rate of liquid to packed column ($l.min^{-1}$)

f_w wetting efficiency

G gas superficial mass flow rate ($kg/m^2.s$)

h height of test section (m)

h_s static liquid holdup (dimensionless)

I_{lim} total intensity of limiting diffusion current (A)

k_1 kinetic rate constant of pseudo first order reaction (s^{-1})

k_d liquid solid mass transfer coefficient ($m.s^{-1}$)

k_{ls} liquid solid mass transfer coefficient ($m.s^{-1}$)

$k_{ls}\phi$ effective liquid solid mass transfer coefficient ($m.s^{-1}$)

$(k_{ls})_c$ chemical liquid solid mass transfer coefficient ($m.s^{-1}$)

$k_{ls}a$ volumetric liquid solid mass transfer coefficient (s^{-1})

k_T apparent first-order rate constant (s^{-1})

k_v true rate constant (s^{-1})

k_{app} apparent rate constant (s^{-1})

L liquid superficial mass flow rate ($kg/m^2.s$)

L_v superficial volumetric liquid flow rate ($m^3/m^2.s$)

n number of contact points (n=6 for a cubic array of spheres)

n_e number of electrons involved in reactions

$\Delta P/Z$ pressure drop per unit bed length ($N.m^{-3}$)

r radial coordinate (m)

R reactor radius (m)

S active liquid solid surface area (m^2)

S_{ext} total geometrical external surface area of catalyst (cm^2)

v_G superficial gas velocity ($m.s^{-1}$)

v_L superficial liquid velocity ($m.s^{-1}$)

V_p total geometric volume of catalyst (cm^3)

Dimensionless groups

Ga Galileo number $\frac{\rho_L^{\,2} g d_p^{\,3}}{\mu_L^{\,2}}$

Re Reynolds number $\frac{\rho_L d_p v}{\mu_L}$

Re_{zG} Modified Reynolds number for gas $\frac{v_G \rho_G}{a_c \mu_G}$

Re_{zL} Modified Reynolds number for liquid $\frac{\mathrm{Re}_L}{\varepsilon_L}$

Sh Sherwood number $\frac{k_{ls} d_p}{D_{iff}}$

Sh_z Modified Sherwood number $\frac{k_{ls} \vartheta_z}{D_{iff}}$

Sc Schmidt number $\frac{\mu}{\rho D_{iff}}$

Greek symbols

α_s fraction of static wetted area

α_t sum of dynamic and static wetted area fractions

α_w physically wetted area fraction

ε bed porosity

ε_B Average bed porosity

ε_L Liquid holdup

η_{CE} external contacting efficiency, fraction of externally wetted area (dimensionless)

η_i fraction of internal volume wetted (dimensionless)

η_T catalyst effectiveness factor (dimensionless)

η_{TB} catalyst effectiveness factor in a trickle bed reactor (dimensionless)

μ viscosity (Pa.s)

ϑ equivalent film thickness $\left(\frac{\mu_L^{\,2}}{g\rho_L^{\,2}}\right)^{1/3}$ (m)

ρ density (kg/m^3)

σ surface tension (N/m)

ϕ fraction of external surface area of packing that is wetted

Φ_T Thiele modulus

Subscripts

1 refers to linear octane hydrogenation reaction (van Houwelingen & Nicol, 2010)

2 refers to isooctene hydrogenation reaction (van Houwelingen & Nicol, 2010)

L liquid phase

G gas phase

w water

Chapter 1 - Introduction

Trickle bed reactors are vital part of petrochemical and chemical industries as they are employed to carry out gas-liquid reactions on a fixed catalytic bed. The co-current downflow of gas and liquid through a trickle bed reactor exhibits complex flow patterns which affect hydrodynamic properties and have a direct effect on the rate of reaction. Industrial trickle bed reactors usually operate in the low interaction trickle flow regime which is characterised by low co-current gas and liquid flow rates where the liquid trickles down in films or rivulets and forms stagnant liquid pockets (Mederos et al, 2009; Lutran et al, 1991; van der Merwe & Nicol, 2009). This distribution of liquid causes partial wetting of catalyst particles and affects the rate of gas-liquid and solid-liquid mass transfer which in turn influences conversion rates in the reactor. Therefore, the role of these factors affecting trickle bed reactor performance should be quantitatively evaluated in laboratory reactors for accurate scale up of data to ensure proper design of the industrial reactor.

It is desired that the laboratory scale reactor be as small as possible while maintaining the accuracy of the data that can be obtained from this reactor. Reducing the length of the reactor will influence the significance of kinetic measurements in lab scale reactors due to changes in either hydrodynamics, if fluid velocities are changed, or the residence time of the reagents as a result of increasing the space velocity to maintain hydrodynamics. Another approach to employ the same superficial velocity as commercial reactors and maintain hydrodynamics is to use pellets in the lab scale reactor although this will require large amounts of feed. Alternatively, the reactor diameter can be reduced without causing major changes in flow patterns and minimise the amount of feed required. However, there is a limit to which the reactor diameter can be reduced due to wall effects on rate controlling hydrodynamic parameters at low column to particle diameter ratios. As a result it is necessary to evaluate the extent the hydrodynamic characteristics of a small diameter reactor differs from a reactor where the wall effects are negligible.

The spatial distribution of liquid in a packed bed is also significantly affected by operating history of the packed bed apart from the operating conditions and flow

regime in which the reactor is operated. This is a result of multiple hydrodynamic steady states occurring in the low interaction regime. This phenomenon of hydrodynamic multiplicity is important as it influences hydrodynamic parameters and complicates prediction of trickle bed reactor performance (Van der Merwe & Nicol, 2005; Loudon et al, 2006; Van Houwelingen, 2006). The effect of multiple states in packed beds is illustrated in the form of hysteresis loops where the hydrodynamic parameter studied is plotted as function of operating history of the bed, in terms of liquid or gas flow rates (Van der Merwe, 2008). The extreme upper and lower boundaries are a result of prewetting procedures applied to the bed and represent the limiting states of hydrodynamic multiplicity. The highest upper branch is attained when the flow rates reach the high interaction regime and then are decreased to the operating point. The lowest branch is attained when operating flows are introduced at an increasing rate into a bed that was previously flooded and subsequently drained. In order to scale up data from small diameter trickle bed reactors with greater accuracy, it is necessary to determine the possible wall effects on hydrodynamic multiplicity by quantification of key hydrodynamic parameters in different hydrodynamic states.

The trickling flow of liquid in the low interaction regime causes partial wetting of catalyst particles and formation of stagnant liquid pockets which results in poor mass transfer of the liquid reagent to the solid catalyst and effective wetting of catalyst by flowing liquid. Most commercial reactors operate in the trickle flow regime in which reactions that are usually liquid limited are carried out. As a result, the transfer of reagent through the liquid film to the solid catalyst and the wetting efficiency of the catalyst are essential hydrodynamic parameters directly influencing the rate of reaction. Previous studies in small diameter trickle bed reactors tend to focus on indirect factors influencing reaction rate which include pressure drop and liquid holdup (Al-dahhan & Dudukovic, 1994; Holub et al, 1993). However, this study will investigate the influence of wall effects on the specific liquid solid mass transfer, which directly affect the rate of conversion in trickle bed reactors. The majority of recent studies employ the electrochemical technique to determine the liquid solid mass transfer coefficient as it is well understood and provides local instantaneous measurement.

Chapter 2 - Literature Survey

2.1 Flow regimes

For gas and liquid concurrent downflow through a packed bed, a variety of flow regimes can be encountered. The flow regimes are categorised into two regimes namely the high interaction regime and low interaction regime based on fluid flow rates. The flow regime map presented in Figure 1, which was prepared by Gianetto & Specchia, (1992) takes into account the results of the vast amount of studies on the downflow operation of reactors. The pulsing, spray and dispersed bubble flow regimes are collectively classified as the high interaction regime. Dispersed bubble flow occurs at high liquid flow rate and low gas flow, as the gas is dispersed as bubbles in the continuous liquid. At high gas flow and low liquid flow, the liquid is entrained in the gas flow and is classified as the spray flow regime. The pulsing regime is encountered at higher liquid and gas mass flow rates. It is characterised by bands of liquid rich regions and gas rich regions which move alternately through the bed as the liquid blocks the channel between the solid particles (Attou et al, 1999). At low liquid and gas mass flow rates the low interaction regime is encountered where liquid trickles down the packing under influence of gravity resulting in complex flow patterns. It is essential to understand the flow regime in which the reactor operates as the fluid flow pattern has an impact on reaction rate.

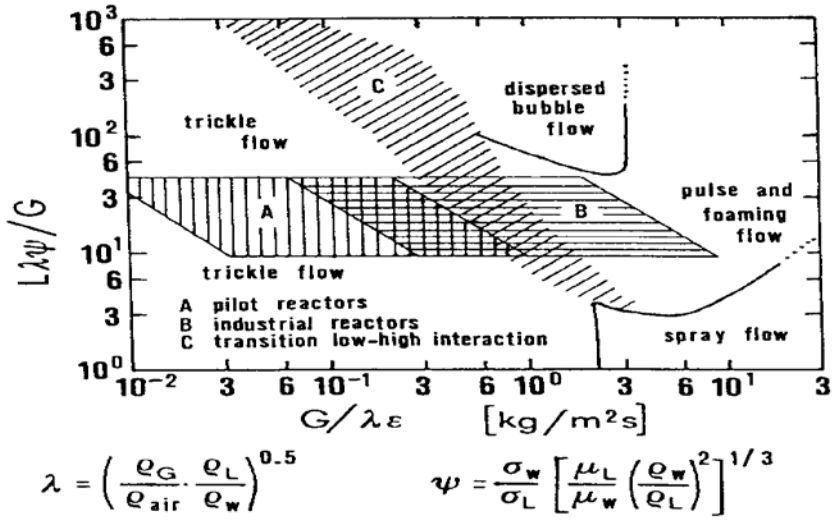

Figure 1: Generalised flow map: downward flow, foaming and non foaming systems. Gianetto & Specchia (1992)

2.1.1 Trickle flow morphology

It is desired that good contact between the gas, liquid and solid phases is attained in a trickle bed reactor. Hence, the liquid distribution in trickle flow regime is important due to the low liquid flow rates. The trickle flow regime can be divided into two regimes namely the partial wetting trickling regime and the complete wetting trickling regime (Lutran et al, 1991). The partial wetting trickling regime is encountered at very low liquid flow rates where a faction of the packed bed is not wetted. Complete wetting trickling regime is attained when the liquid flow rate is increased to an extent where the packed bed is totally wetted. In the low interaction regime, Christensen et al (1986) identified that the liquid flows as films, rivulets and less frequently as drops through the catalyst bed. Figure 2 demonstrates the rivulet and film flow on a particle scale and Figure 3 on a bed scale.

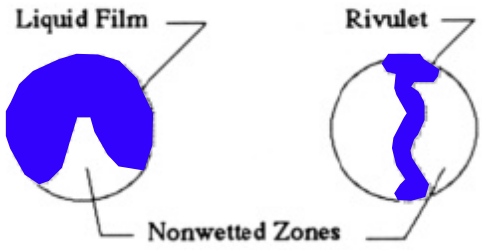

Figure 2: Schematic representation of film flow and rivulet flow on a particle scale in the trickle flow regime (Lutran et al, 1991)

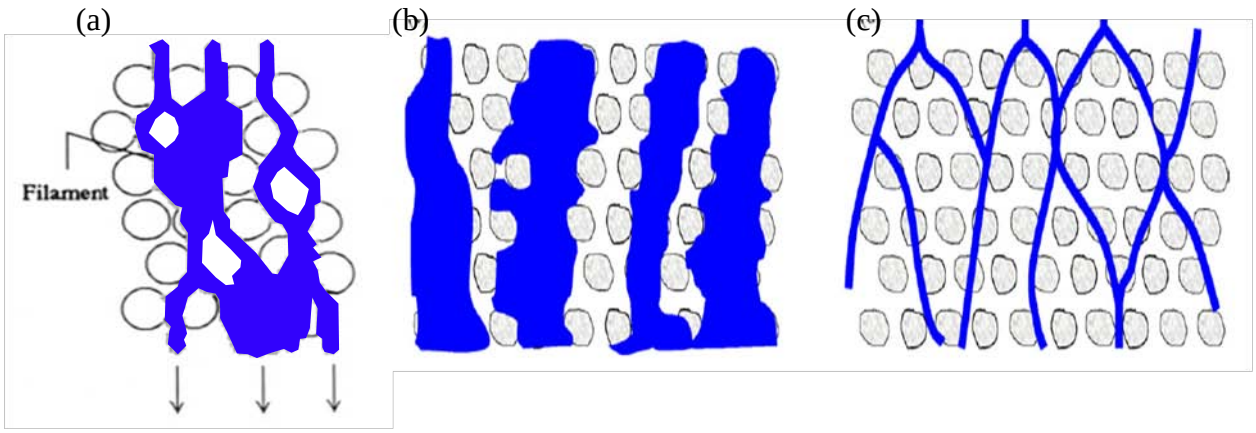

Figure 3: Schematic representation of (a) filament, (b) film and (c) rivulet flow on a bed scale (Mederos et al, 2009; Lutran et al, 1991)

These flow patterns are a result of the interconnection of a series of pores or voids in the bed each filled with a fraction of liquid. Rivulet flow, as depicted in Figure 3(c), is idealised to be result of the intersection of pores with high liquid fractions together with pores of very low liquid fractions and film flow the connection of pores with low yet similar liquid fractions (van der Merwe & Nicol, 2009). In film flow, the packing surface is either completely or partially covered by a film of liquid of varying thickness while gas moves in the interstitial void space, as illustrated in Figure 3(b). A filament, illustrated in Figure 3(a), is a stream of liquid formed by collection of liquid pockets that fill multiple void spaces. Film flow is desired for liquid limited reactions as it results in greater contact between the liquid and solid and more efficient use of the packed bed. The maldistribution of liquid illustrated in Figures 2 and 3 is usually attained in the trickle flow regime, when liquid is driven by gravity rather than frictional forces (Mederos et al, 2009). However, at high gas superficial velocities the effect of gas drag on liquid flow becomes significant and tends to spread the liquid, resulting in thinner films. Each unique liquid flow distribution in the trickle flow regime corresponds to a specific hydrodynamic state which influences the value of the hydrodynamic parameters that characterise the packed bed. The manifestation of a particular liquid distribution and the resulting flow pattern is chiefly attributed to the operating history of the packed bed, especially with regards to prewetting procedure applied, apart from the operating fluid velocities. Therefore, multiple hydrodynamic states can exist, where the hydrodynamic parameters can adopt different values at the same operating conditions for various prewetting procedures applied (Van der Merwe & Nicol, 2005; Loudon et al, 2006; Van Houwelingen, 2006; Maiti, 2006).

2.1.2 Hydrodynamic Multiplicity

The existence of multiple hydrodynamic steady states, otherwise known as hydrodynamic multiplicity, was first observed by Kan & Greenfield (1978). Multiple hydrodynamic states are only possible in the low interaction trickle flow regime as the flow patterns in the high interaction regimes are transient. The term ‘hydrodynamic multiplicity’ refers to the effects of prewetting procedures as well as operating history of the bed, with regard to fluid flow rates, on hydrodynamic parameters. It is usually presented in the form of hysteresis loops where one operating condition (usually gas or liquid velocity) is varied while the others are kept

constant as shown in Figure 4. In this figure it was observed that the hydrodynamic parameter, pressure drop, increases with liquid velocity (while keeping the gas velocity constant) from point 1 to point 2. When the liquid velocity is decreased back to its starting point the pressure drop at point 3 is higher than that initially obtained at point 1 for the same liquid velocity. The bottom branch of the hysteresis loop was obtained by increasing the liquid flow rate to the pulsing regime and the highest upper boundary was obtained by subsequently decreasing the flow from the pulsing regime to the starting point. These two branches represent the limiting cases of hydrodynamic multiplicity and can also be attained by applying prewetting procedures to the bed prior to establishing flows at their operating velocities. The upper boundary refers to Levec prewetting, as it was first applied by Levec et al (1986) and the lower boundary to Kan prewetting which was first applied by Kan & Greenfield (1978). A short description of the prewetting procedures they represent is given below.

- Levec prewetted bed

  A dry catalyst bed is flooded with liquid until the catalyst particles are thoroughly prewetted. The reactor is then drained completely under gas flow before gas and liquid flows are introduced into the reactor at their operating velocities.

- Kan prewetted bed

  The fluid flow rates are increased until the pulsing flow regime is reached. Thereafter the fluid flow rates are reduced gradually to the operating flow rates.

This phenomenon of hydrodynamic multiplicity is closely associated with liquid distribution in the bed as different hydrodynamic states result in differences in liquid flow structure and distribution (Van der Merwe & Nicol, 2005). The studies of liquid distribution in the trickle flow regime revealed that rivulet flow is dominant in a Levec prewetted bed whereas film flow is present in a Kan-liquid bed (Lutran et al, 1991; Christensen et al, 1986; van der Merwe, 2008). The effect of hydrodynamic

multiplicity on hydrodynamic parameters is important in order to model the fluid flows and reaction yield of a trickle bed reactor accurately.

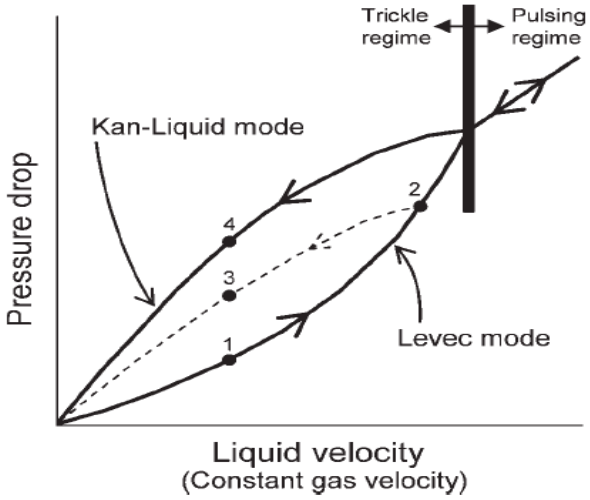

Figure 4: Typical hysteresis behaviour for pressure drop (Van der Merwe, 2008)

2.2 Key hydrodynamic parameters for liquid limited reactions in trickle bed reactors

The hydrodynamics of the trickle flow regime are investigated by measuring hydrodynamic parameters in terms of operating conditions (temperature, pressure and fluid velocities), fluid properties, and particle and bed characteristics. The evaluation of hydrodynamic parameters is essential for the optimal design of trickle-bed reactors as they have an impact on the conversion, yield and selectivity of reactions apart from the reaction kinetics, operating temperature and pressure. The most commonly encountered hydrodynamic parameters are liquid holdup, wetting efficiency and two-phase pressure drop, volumetric liquid solid mass transfer coefficient, volumetric gas liquid mass transfer coefficient, liquid phase axial dispersion and liquid maldistribution factor. Some of these hydrodynamic parameters will have a more direct influence on the reaction rate and optimal reactor performance depending on the application of the trickle bed reactor. The reactions that take place in an industrial trickle bed reactor are usually liquid limited where the transport of liquid to the catalyst surface limits the rate of the reaction. For this application, the key hydrodynamic parameters influencing optimal liquid solid contact, liquid solid mass transfer rate and consequently the reaction rate will be the

liquid solid mass transfer coefficient and wetting efficiency. It is desired that all the catalyst particles are completely irrigated by flowing liquid to ensure proper utilisation of the catalyst and a high conversion rate. Hence, a good understanding of liquid solid mass transfer as well as wetting efficiency is required to model industrial reactors operated in the trickle flow regime accurately.

2.2.1 Liquid solid mass transfer

The transfer of reagents through the liquid film to the solid catalyst is essential in the trickle flow regime for liquid limited reactions. The liquid solid mass transfer coefficient is an important parameter for the design and operation of trickle bed reactors since the volumetric gas liquid mass transfer coefficient is generally slightly higher than the volumetric liquid solid mass transfer coefficient (Gianetto & Specchia, 1992). There have been numerous correlations published for the prediction of liquid solid mass transfer coefficients in trickle bed reactors (Sims et al, 1993; Larachi et al,2003; Satterfield et al, 1978; Gabitto & Lemcoff, 1987; Baussaron et al, 2007a; Jolls & Hanratty, 1969). The majority of studies reviewed employed the electrochemical technique to measure mass transfer coefficients. However, some studies employ the dissolution technique (Satterfield et al, 1978; Baussaron et al, 2007) and a chemical reaction technique (van Houwelingen and Nicol, 2010). Table 1 summarises some of the previous studies of liquid solid mass transfer reviewed and lists the correlations proposed by some of the studies. The mass transfer coefficient for all the flow regimes is correlated according to the following general equation in terms of dimensionless numbers:

$$Sh\phi Sc^{-a} = b\,\mathrm{Re}^{c} \tag{1}$$

Where the Reynolds number, Re, represents the influence of liquid flow rate in single phase flow and gas or liquid flow rates in the case of two phase flow. This form of correlating mass transfer coefficient is preferred as it takes into account physicochemical properties of the fluids and facilitates the direct comparison with results from other studies. If more than one packing size or type is compared then the coefficient for bed porosity, ε, is considered as part of the group on left hand side of equation 1 (Bartelmus, 1989).

Table 1: Summary of liquid solid mass transfer studies

Reference	Technique	Flow regime	Packing	D/d_p	Correlation	Condition
1. Bartelmus (1989)	Electrochemical	Flooded, trickle, pulse	3.86 & 6.32 mm spheres	11.9-19.4	$\varepsilon Sh = 0.798\,\mathrm{Re}_L^{0.51}\,Sc^{0.33}$ $Sh_z / Sc^{0.33} = (1.19 + 0.0072\,\mathrm{Re}_{zG})^{1.1}(\mathrm{Re}_{zL})^{0.494}\,Ga^{-0.22}$ $Sh_z / Sc^{0.33} = 2.269(\mathrm{Re}_{zL})^{0.494}(\mathrm{Re}_{zG})^{0.178}\,Ga^{-0.276}$	Flooded Trickle Pulse
2.Baussaron et al (2007a)	Dissolution of naphthol	partial wetting	3mm spheres	16.7	$\phi Sh = 8.58x10^{-4}\left(\frac{\mathrm{Re}_L}{\varepsilon_L}\right)^{1.91} Sc_L^{1/3}$	
3. Chou et al (1979)	Electrochemical	pulse	7.8 mm spheres	19.5	$\phi Sh = \frac{0.72\,\mathrm{Re}_L^{0.54}\,\mathrm{Re}_G^{0.16}\,Sc^{1/3}}{\varepsilon}$	$40<\mathrm{Re}_G<300$ $50<\mathrm{Re}_L<140$
4. Delaunay et al (1982)	Electrochemical	trickle & pulse	4 mm			
5. Jolls & Hanratty (1969)	Electrochemical	trickle & pulse	1in spheres	12	$ShSc^{-1/3} = 1.64\,\mathrm{Re}^{0.6}$ $ShSc^{-1/3} = 6.4\,\mathrm{Re}^{0.5}$	Re<35 Re>1120
6. Satterfield et al (1978)	Dissolution of Benzoic acid	trickle & pulse	3mm & 6mm cylinders	11.7-23.3	$\phi ShSc^{-1/3} = 0.815\,\mathrm{Re}_L^{0.822}$	Re<60
7. Sims et al (1993)	Electrochemical	trickle & pulse	2x3mm extrudates	24.2	$\phi Sh = 5.4\,\mathrm{Re}_L^{0.44}\,Sc^{1/3}$	pulsing regime
8.Trivizadakis & Karabelas (2006)	Electrochemical	Pulse	6mm spheres 1.5x3.1 mm cylinders	23.3-63.1	$Sh = 0.35\,\mathrm{Re}_L^{0.6}\,Sc^{1/3}$	for induced pulsing

This parameter compensates for changes in porosity due to wall effect which is prominent in small diameter columns. Although none of the studies presented in Table 1 focused on wall effects on the liquid solid mass transfer coefficient, the column to particle diameter ratio employed in each of the studies is reported.

2.2.1.1 Comparison of Liquid solid mass transfer correlations

The correlations for liquid solid mass transfer coefficients from various studies are presented in Figure 5. The reasons for variation between studies for mass transfer coefficient are listed below:

- Entrance and exit effects
- The different rates of wall flow
- Wetting of the particles
- Measurement technique

Chou et al (1979) reported that the change of pellet size and void fraction of the bed due to the dissolution of particles could have had an effect on the results obtained from previous studies.

- Packing diameter

An increase in packing diameter, d_p, leads to higher liquid solid mass transfer values (Delaunay et al, 1982).

- Differences in interfacial area for liquid solid mass transfer

The liquid solid interfacial area for mass transfer depends on physicochemical properties of the liquid phase and geometric characteristics of the packing (Delaunay et al, 1982).

- Reporting of integral volume averaged mass transfer coefficients

Chou et al (1979) reported that the use of integral volume averaged mass transfer coefficients is risky close to the transition region. As axial pressure reduction increases the down flow gas velocity such that two flow regimes may coexist in the packed bed; spray flow at the top and pulsing at the bottom. As a

result, they reported local effective mass transfer coefficients in fully developed flow.

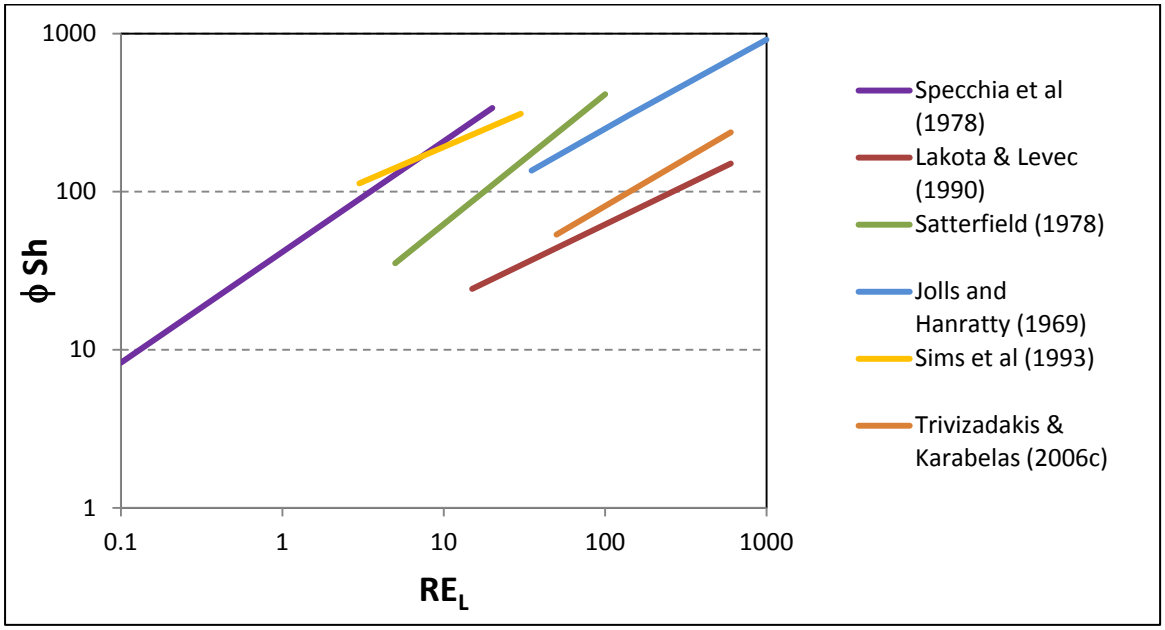

Figure 5: Liquid solid mass transfer coefficient predictions from literature studies

2.2.1.2 Effects of Hydrodynamic multiplicity on liquid solid mass transfer

The electrochemical method cannot measure the actual liquid solid mass transfer coefficient, k_{ls}, independently from the fraction of wetted solid area, f_w. Hence, results from studies are compared using an effective mass transfer coefficient, $k_{ls}\phi$ or modified Sherwood number, ϕSh. Satterfield et al (1978) reported that the trickle flow regime outperforms flooded and attribute the increase in the effective mass transfer to the increase of interstitial velocity due to a decrease in holdup despite a decrease in wetting efficiency. This result confirmed the work of Baussaron et al (2007a) which indicated that wetting efficiency only impacts the liquid solid interfacial area and does not influence liquid solid mass transfer conductance which depends on liquid interstitial velocity. However, recent studies on the effect of hydrodynamic multiplicity on liquid solid mass transfer have shown that the Kan prewetted bed which has higher holdup (lower interstitial velocities) yielded higher values than the Levec prewetted bed with lower holdup (higher interstitial velocities) (Joubert & Nicol, 2009; Sims et al 1993, van Houwelingen & Nicol, 2010). This effect of hydrodynamic multiplicity is attributed to the higher wetting efficiencies in the Kan prewetted bed (Sims et al, 1993) and different liquid flow structures in the Kan and Levec prewetted beds (van Houwelingen & Nicol, 2010). Therefore, hydrodynamic multiplicity in the

trickle flow regime can have a significant yet complex impact on rate determining parameters.

2.2.1.3 Spatial variation of liquid solid mass transfer

The non-uniform distribution of liquid and gas flows in the interstitial spaces during trickle flow will result in a substantial variation in local mass transfer rates. The majority of studies on the electrochemical measurement of local liquid solid mass transfer coefficients report correlations based on time averaged measurements using a single sphere electrode in a packed bed (Trivizadakis & Karabelas, 2006c; Chou et al, 1979). As a result, the local conditions of the equipment were not sampled accurately and the spatial variation of local mass transfer rates in the packed bed was not considered. Chou et al (1979) found that the time averaged effective Sherwood number ϕSh depends on its location in the packed bed in the gas continuous regime. Trivizadakis & Karabelas (2006c) reported a large spread (almost two orders of magnitude) in local Sherwood numbers due to variations in local packing which resulted from non uniform phase distribution. Jolls & Hanratty (1969) observed no radial variation of mass transfer coefficient on moving the particle from the center of the packed bed to the wall of column when the Reynolds number was greater than 35. However, when the Reynolds number was less than 35 the mass transfer rates at locations closer to the wall ($r/R>0.75$) were higher and were more independent of flow rate than the locations closer to the center of the column. This result infers the possibility of wall effects on the liquid solid mass transfer coefficient. The overall mass transfer coefficient was also determined by some researchers (Bartelmus, 1989; Giabatto & Lemcoff, 1987; Trivizadakis & Karabelas, 2006c) by placing single electrode spheres at different positions along the axis of the column. However, recent studies employ a multiple packing electrode which consists of a section of multiple active spheres in a packed bed acting as the cathode (Delaunay et al, 1982, Joubert & Nicol, 2009). An advantage of using the multiple packed electrode section is that the effect of radial dispersion does not influence the measurement of mass transfer coefficient (Delaunay et al, 1982). Chou et al (1979) performed preliminary electrochemical experiments at various axial locations in a 1.35 m packed bed to determine the regions of the packed bed where

end-effects exist. They found that end effects were prevalent at the entrance at a distance of 75 cm from the top and at the exit at 20 cm from the bottom under pulse flow conditions. This investigation suggested that measurements taken in short beds may be compromised by these end effects. The spatial variability of effective mass transfer coefficients indicates that the catalyst particles are incompletely wetted at low liquid flow rates.

2.2.2 Wetting Efficiency

Incomplete wetting of the solid catalyst particles in a trickle bed reactor occurs when the low gas and liquid flows encountered in the trickle flow regime are insufficient to ensure complete coverage of all pellets in the bed with a continuous liquid film. The wetting efficiency of the catalyst particles is expressed as the fraction wetted external area per total external surface area of the catalyst particle. This is a critical parameter for proper scale up of laboratory reactors as it impacts gas-solid and liquid solid mass transfer areas. This in turn influences the catalyst effectiveness (η_T) by affecting the apparent diffusivity in the internal area of porous catalysts which has an effect on the effectiveness of a trickle bed reactor (η_{TB}) compared to an ideal plug flow reactor. Dudukovic, (1977) derived a formula (see Table 2) for the liquid limited trickle bed reactor effectiveness factor based on partially wetted porous catalyst particles. The partially wetted particles were modelled as irregular shaped particles where the catalyst effectiveness (η_T) is a function the Thiele modulus Φ_T. The value of Thiele modulus Φ_T, determines whether incomplete external or internal wetting affects the catalyst effectiveness factor to a greater extent. For large values of Thiele moduli, fraction of external area wetted (η_{CE}) is the dominant parameter, whereas for small values of Φ_T, fraction of internal volume wetted η_i is more important. It is important to note that effective external wetting is different from total physical external wetting due to stagnant liquid zones with low liquid renewal that do not contribute much to mass transfer (Sicardi et al, 1980). Hence, the wetted area can be divided up into a dynamic area, in contact with flowing liquid, and a static area which is in contact with semistagnant liquid. Sicardi et al, (1980) determined the static wetted area of spherical particles from static holdup, h_s (see Table 2). A large spread in wetting efficiency data from the various studies was noted which could be

attributed to trickle flow hydrodynamics, the different measurement techniques and operating conditions specific to each study as well as only recent awareness of hydrodynamic multiplicity arising from prewetting procedures.

2.2.2.1 Comparison of wetting efficiency transfer correlations

The main experimental methods employed in previous studies to measure the external wetting efficiency are a dynamic tracer method (Colombo et al, 1976; Sicardi et al, 1980; Al-Dahhan & Dudukovic, 1995), chemical reaction method (Satterfield, 1975; Specchia et al, 1978; Llano et al, 1997, van Houwelingen & Nicol, 2010), magnetic resonance imaging (Sederman & Gladden, 2001) and colorimetric method (van Houwelingen et al, 2006; Lazzorini et al, 1988; Bassuron et al, 2007). Table 2 lists the reported correlations from previous studies and the experimental method employed. The basis of many of the wetting efficiency studies involved the comparison of a trickle bed reactor to a liquid filled reactor or slurry reactor where there is total wetting of the particles. Satterfield (1975), specified that the reaction rate constant obtained from trickle bed reactor should be referred to as the apparent rate constant k_{app}, whereas the rate constant obtained from a slurry reactor, k_v referred to as the intrinsic reaction rate constant. He found k_{app} approaches k_v with an increase in liquid flow. The chemical reaction method essentially involves comparing the reaction rates of a trickle bed reactor with a liquid filled reactor. An adaption of this method was used by van Houwelingen & Nicol (2010), to determine wetting efficiency from conversion data obtained from two liquid-limited reactions taking place in parallel in the reactor. The majority of early studies on wetting efficiency employed the dynamic tracer technique. This technique compares the tracer response from a liquid filled reactor with a trickle bed reactor. Colombo et al (1976) employed this technique and interpreted wetting efficiency in terms of apparent internal diffusivity (see table 2) where they reasoned that catalyst efficiency factors (η_{CE}) and apparent reaction rate constant from a trickle bed reactor, k_{app} can be affected by variations of apparent internal diffusivity. Therefore, the ratio of internal diffusivities, obtained from the first moments of tracer response curves, was used to determine the wetting efficiency. Sicardi et al (1980) followed from the work

Table 2: Summary of wetting efficiency correlations

Reference	Measurement Technique	Correlation	Comment
1. Dudukovic (1977)		$\eta_{TB} = \eta_{CE} \dfrac{\tanh\left(\dfrac{\eta_i}{\eta_{CE}}\phi_T\right)}{\phi_T}$	Thiele modulus Φ_T for a first order reaction is: $\phi_T = \dfrac{V_P}{S_{ext}}\sqrt{\dfrac{k_v}{D_i}}$
2. Sicardi et al (1980)	Dynamic Tracer	$h_s = \dfrac{\left[2(1-2\alpha_s/n)^3 - 3(1-2\alpha_s/n)^2 + 1\right](1-\varepsilon)n}{4}$	Static holdup used to compute static wetted area
3. Satterfield (1975)		$f_w = \dfrac{k_{app}}{k_v}$	
4. Van Houweligen and Nicol (2010)	Chemical Reaction	$f_w = \left.\dfrac{k_{T1}k_{T2}}{k_{T1}-k_{T2}}\right\|_{Trickle} x \left.\dfrac{k_{T1}-k_{T2}}{k_{T1}k_{T2}}\right\|_{Upflow}$	
5. Colombo et al (1976)	Dynamic Tracer	$f_w = \dfrac{(D_i)_{trickle}}{(D_i)_{flooded}} = \dfrac{(D_i)_{app}}{D_i}$	
6. Sicardi et al (1980)	Dynamic Tracer	$\alpha_w = \dfrac{a_w}{a_T} = \sqrt{\dfrac{(D_i)_{app}}{D_i}}$	
7. Al-Dahhan and Dudukovic (1995)	Dynamic Tracer	$\eta_{CE} = 1.104\,\mathrm{Re}_L^{1/3}\left\{\dfrac{1+\left[(\Delta P/Z)/\rho_L g\right]}{Ga_L}\right\}^{1/9}$	$\mathrm{Re}_L = \dfrac{v_L \rho_L d_p}{\mu_L(1-\varepsilon)}$, $Ga_L = \dfrac{{d_p}^3 {\rho_L}^2 g\varepsilon^3}{{\mu_L}^2(1-\varepsilon)^3}$
8. Lakota and Levec (1990)	Dissolution	$f_w = \left[\dfrac{(k_{ls}a)_{two-phaseflow}}{(k_{ls}a)_{\sin gle-phaseflow}}\right]$	
9. Specchia et al (1978)	Dissolution	$(k_{ls}a_s)_c = \sqrt{(k_{ls}a_s)^2 + {a_s}^2 D_{iff} k_1}$	Solved simultaneously with $(k_{ls}a_s)_c = \dfrac{v_L c_o}{hc_i}$
10. Larachi et al (2001)		$f_w = 0.83S + 0.17$ where $S = \dfrac{1}{1+\exp-\sum_{j=1}^{8}\omega_j\left[\dfrac{1}{1+\exp-\sum_{i=1}^{6}\omega_{ij}U_i}\right]}$	The weighting factors, ω_{ij} and normalized input groups, U_i are presented in Larachi et al (2001).

of Colombo et al (1976) calculated the total wetted area from apparent internal diffusivities through the definition of Thiele modulus Φ_T. Al-Dahhan & Dudukovic (1995) employed a tracer technique but used reactor modelling to analyse tracer responses to develop a comprehensive correlation for external partial wetting related to reactor pressure, pressure drop, liquid holdup and gas and liquid flow rates. Apart from the comparison of reaction rates in trickle flow and liquid filled reactors, the volumetric liquid solid coefficients from these two reactors can also be measured. Lakota and Levec (1990) defined wetting efficiency from the comparison of the volumetric mass transfer coefficients ($k_{ls}a$) obtained, using a dissolution technique, in two phase flow to single liquid phase flow at the same interstitial liquid velocities. A similar method was employed by Specchia et al (1978), who calculated wetting efficiency from volumetric liquid solid mass transfer measurements coupled with a pseudo-first-order reaction in the liquid phase. In an attempt to formulate a general expression for wetting efficiency, Larachi et al (2001) gathered a database of wetting efficiency measurements from 14 studies and formulated a correlation following dimensional and statistical analysis of the database. The most informative and accurate data on wetting efficiency were obtained from studies that employed the colorimetric method. The general method involves using a dye colorant in the liquid phase that colours the external surface of particles in contact with the liquid. Thereafter the coloured particles are analysed by various image processing techniques to determine the wetted area and subsequently the wetting efficiency. Baussaron et al (2007c) compared this technique with the tracer method and found that tracer method under predicts wetting efficiency by as much as 20%.

2.2.2.2 Effects of Hydrodynamic multiplicity on wetting efficiency

Van Houwelingen et al (2006) applied the colorimeteric method to determine the particle wetting distributions for two prewetting procedures. They discovered that hydrodynamic multiplicity affects the wetting efficiency since the Kan prewetted bed yielded higher values than a Levec prewetted bed. The different particle wetting distributions obtained for the different prewetting procedures illustrate that different flow patterns are present for each prewetted mode. This was confirmed by channelling which was observed in the Levec prewetted bed but not in the Kan prewetted bed by van Houwelingen et al (2007). Lazzoroni et al (1988) also

employed this method to determine wetting efficiencies and discovered effects of hydrodynamic multiplicity where super prewetting (flooding the bed with liquid and subsequent draining at the desired operating liquid flow rate) exhibited higher values than a non prewetted bed. They also noticed that the radial distribution of wetting efficiency was distorted by gas flow where the wetting in the central section increased while it decreased in the outer section closer to walls.

Although a considerable amount of external wetting efficiency correlations are available literature, there is no general recommended prediction method to model this important hydrodynamic parameter due to their restricted validity of the correlations to the operating conditions and procedures specific to each study.

2.3 Scaling down reactors

The research and development of new processes or optimisation of current processes involving reactors usually requires scaling down of commercial reactors to laboratory reactors. The lab scale reactor should be as small as possible since it is safer and cheaper to operate as it requires less feedstock and catalyst. It is vital that the data obtained from the laboratory reactor can be accurately scaled up to predict performance of a commercial scale reactor. A commercial reactor can be scaled down by two dimensions either, the reactor length or diameter. Two approaches can be followed when scaling down the length of a reactor: maintenance of bed hydrodynamics, or the weight velocity of the reactants. In order to maintain the bed hydrodynamics of the shorter laboratory reactor, the fluid velocities should be kept the same as the commercial reactor which will increase the weight velocity. However, the weight velocity of reactants in a shorter reactor can be sustained by decreasing the fluid velocities such that the space velocity is the same as a commercial reactor though changing the hydrodynamics of the catalyst bed.

A more favourable technique to scale down a reactor is to reduce the reactor diameter as it does not cause significant changes to flow patterns and minimises the bulk feed required to employ the same fluid velocities as a commercial reactor. However, there is a limit to which the reactor diameter can be reduced due to wall

effects at low column to particle diameter (D/d_p) ratios. These wall effects are characterised by the channelling of liquid at the reactor wall due to higher porosity close to the wall. As a result, wall effects have the potential for affecting hydrodynamic parameters influencing conversion rate in trickle bed reactors. A range of column to particle diameter ratio limits has been reported by numerous studies in order to ensure optimal reactor efficiency. However, these ratios are impractical especially when catalyst pellets are used as it necessitates a larger reactor diameter. Therefore, it is necessary to determine the extent to which hydrodynamic parameters that influence the reaction rate differ in small diameter reactors from laboratory reactors without wall effects.

2.3.1 Wall effects

The majority of research done in low column to particle diameter ratio trickle bed reactors tends to focus on radial voidage variation and liquid distribution (Kundu et al, 2001; Sahora et al, 1998; Patwardhan & Pataskar, 1982; Fahien & Stankovic, 1979). The numerous experimental and modelling studies on radial voidage profiles discovered an oscillatory radial voidage profile which dampened with increasing distance from the wall until a steady value was obtained at approximately 4 to 6 particle diameters away from the wall in the case of large diameter beds ($D/d_p > 20$) (Attou et al, 1999; Govindaro & Froment, 1986; Ridgway & Tarbuck, 1968; Sie & Krishna, 1998; Marivoet et al, 1974; Niu et al, 1996; de Klerk, 2003). However, the radial voidage variation close to the wall is quite pronounced compared to the region closer to the center of the bed. This trend is termed the wall effect and is quite prominent in columns with a low column-to-particle diameter ratio as illustrated in figure 6. The wall effect on the average bed voidage is illustrated in figure 7 using the average bed voidage models proposed by de Klerk (2003) and Benyahia & O'Neill (2005).

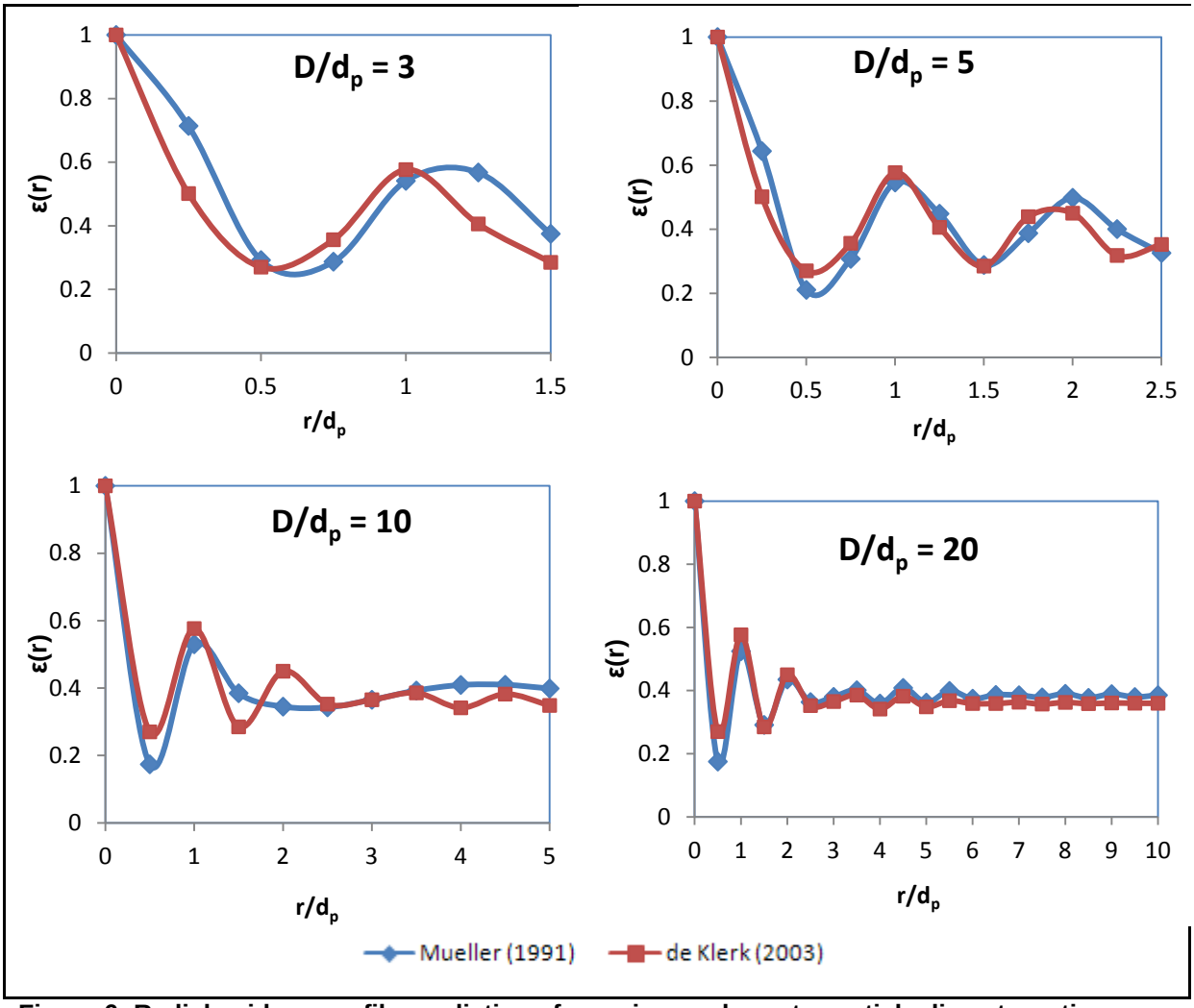

Figure 6: Radial voidage profile predictions for various column-to-particle diameter ratios

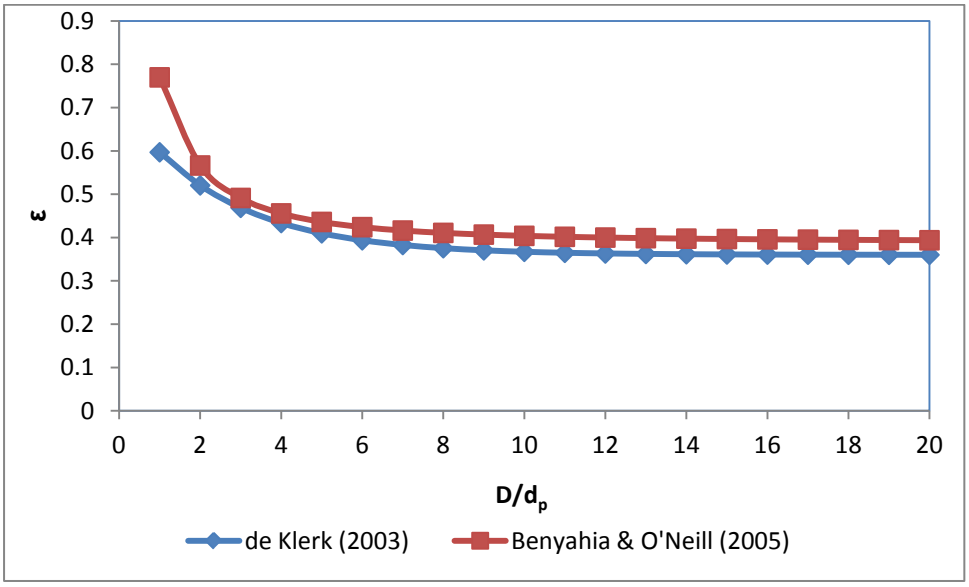

Figure 7: Average bed voidage predictions as a function of column-to-particle diameter ratios

The wall effect on average bed voidage appears to be minimal at a column-to-particle diameter ratio greater than 10 according to figure 7. The large voidage close to the wall results in higher average bed porosity in columns with column-to-particle diameter ratios less than 10, as shown in figure 7.

Table 3: Comparison of center bed porosity and average bed voidage for various column-to-particle diameter ratios

D/d_p	ε de Klerk (2003)	ε (r) de Klerk (2003)	ε (r) Mueller (1991)	Standard Deviation
3	0.469	0.285	0.375	0.092
5	0.410	0.352	0.326	0.043
10	0.367	0.348	0.399	0.025
20	0.360	0.360	0.385	0.015

A comparison of the predicted average bed voidage and the radial porosities at the center of the bed for column-to-particle diameter ratios of interest are illustrated in Table 3. The deviation of the average bed voidage from the voidage at the bed center is greater for $D/d_p \leq 10$, while at $D/d_p = 20$ there is little deviation between the average and bed center voidage predictions. This further illustrates that the wall effect is prominent in columns with $D/d_p \leq 10$.

The increase in bed porosity with a decrease in the column to particle diameter ratio has been found to impact the wetting efficiency due to less contact points between particles to sustain liquid flow patterns (Julcour-Lebigue et al, 2009). The large voidage close to the column wall also causes the liquid phase to preferentially channel along the wall of the reactor which results in a reduction of interfacial area for mass transfer of the reagents to the catalyst (Sie & Krishna, 1998). However, the wall surface retards the flow and as result a radial velocity profile is more irregular at low column to particle diameter ratios (Sie & Krishna, 1998). This irregular velocity profile will result in a spread in residence time for a reactant and will consequently impact the temperature and concentration profiles in the reactor. Hence, it can be inferred that the efficiency of a small diameter trickle bed reactor may be related to the ratio of column to particle diameter ratio (D/dp).

The studies on liquid distribution in small diameter columns found that wall flow development reaches an equilibrium value fairly rapidly (Satterfield, 1975;

Templeman & Porter, 1965). Hence equilibrium liquid flow distributions were used in these studies to determine the critical column to particle diameter. The equilibrium liquid flow distribution was attained when the wall flow was not a significant fraction of the total liquid flow and the radial distribution of liquid flow was considered uniform over the cross-sectional area of the reactor. A few researchers analysed the influence of low column to particle diameter ratios on reactor performance by evaluating parameters associated with the modelling of fluid flow in small diameter trickle bed reactors (Attou et al, 1999; Onda et al,1973).

Table 4: Summary of recommended minimum column to particle diameter ratios from literature

Reference	Min D/d_p	Conditions
Baker et al (1935)	> 8	For large irregular solid packing and regular solid packing spheres in absorption columns
Hoftyzer (1964)	>10	To avoid influence of wall on position of dumped packing
Templeman and Porter (1965)	>8-12	To prevent liquid flow to wall
Mears (1971)	>4	To attain isothermality
Butt and Weekman (1974)	>10-20	To control radial temperature gradients
Satterfield (1975)	>10	Reduce hydrodynamic problems associated with wall flow
Herskowitz and Smith (1978)	>18	Gas continuous and trickling flow regimes, air-water, D/d_p<30, catalyst particle sizes from 0.26 to 1.1cm with granular, spherical and cylindrical shapes
Gierman (1988)	>16	To avoid wall flow
Larachi et al (1991)	>11.5	For particles of 2mm diameter
Al-Dahhan and Dudukovic (1994)	>20	For uniform liquid distribution
Sie and Krishna (1998)	>20	From average bed porosity and permeability variations with D/dp
Attou et al (1999)	>12-14	Cocurrent gas-liquid flow, trickle flow regime, 0.1-10MPa
Perego and Pertello (1999)	>25	To prevent wall effect from being significant

Most of the earlier studies on liquid distribution and critical column to particle diameter ratios were focused on packed absorbers and distillation columns. As a result, the columns were packed with larger and irregular catalyst shapes rather than smaller uniformly sized catalyst particles employed in trickle bed reactors (Baker et

al, 1935; Hoftyzer, 1964; Templeman & Porter, 1965). Hence, there is a wide variation in the limiting values of the column to particle diameter ratio from various authors as illustrated in the table 4. Attou et al, (1999) found a discrepancy between their theoretical model prediction and experimental results for pressure gradient and liquid hold up when the column to particle diameter ratio was below 12. They attributed this difference to the incapability of the model to predict channelling of liquid flow, due to the higher local porosities at reactor wall at low column to particle diameter. A significant error in model predictions for pressure drop and liquid holdup data in trickle bed reactors with D/dp<20 due to the wall effects on liquid distribution was also realised by earlier studies (Holub et al, 1993; Al-Dahhan & Dudukovic, 1994). However, no study has been conducted to evaluate the wall effects on two key hydrodynamic parameters directly influencing reaction rate namely, liquid solid mass transfer and wetting efficiency, in low column to particle diameter trickle bed reactors.

Chapter 3 - Objectives

The primary objective of this study is to analyse the effect of low column-to-particle-diameter ratios on the effective liquid solid mass transfer coefficient ($k_{ls}\Phi$). Therefore, $k_{ls}\Phi$ will be measured, using the electrochemical technique, in trickle bed reactors with column to particle diameter ratios ranging from 10 to 1.

The secondary objective of this study is to investigate the effect of hydrodynamic multiplicity on $k_{ls}\Phi$ in columns with low column-to-particle diameter ratios. The limiting cases of hydrodynamic multiplicity that will be explored are Kan, Levec (with and without gas flow) and Super bed prewetting procedures.

Chapter 4 - Experimental

3.1 Experimental Setup

The objective of this study was to investigate the effect of small column to particle diameter ratios on liquid solid mass transfer in a trickle bed reactor operated in the low interaction regime. An effective specific liquid solid mass transfer coefficient, $k_{ls}\phi$, was measured in a range of different column diameters by employing an electrochemical technique. Two experimental setups were used in this study in order to enable measurements from a range of column sizes. The process flow diagrams for the experimental setups are given below:

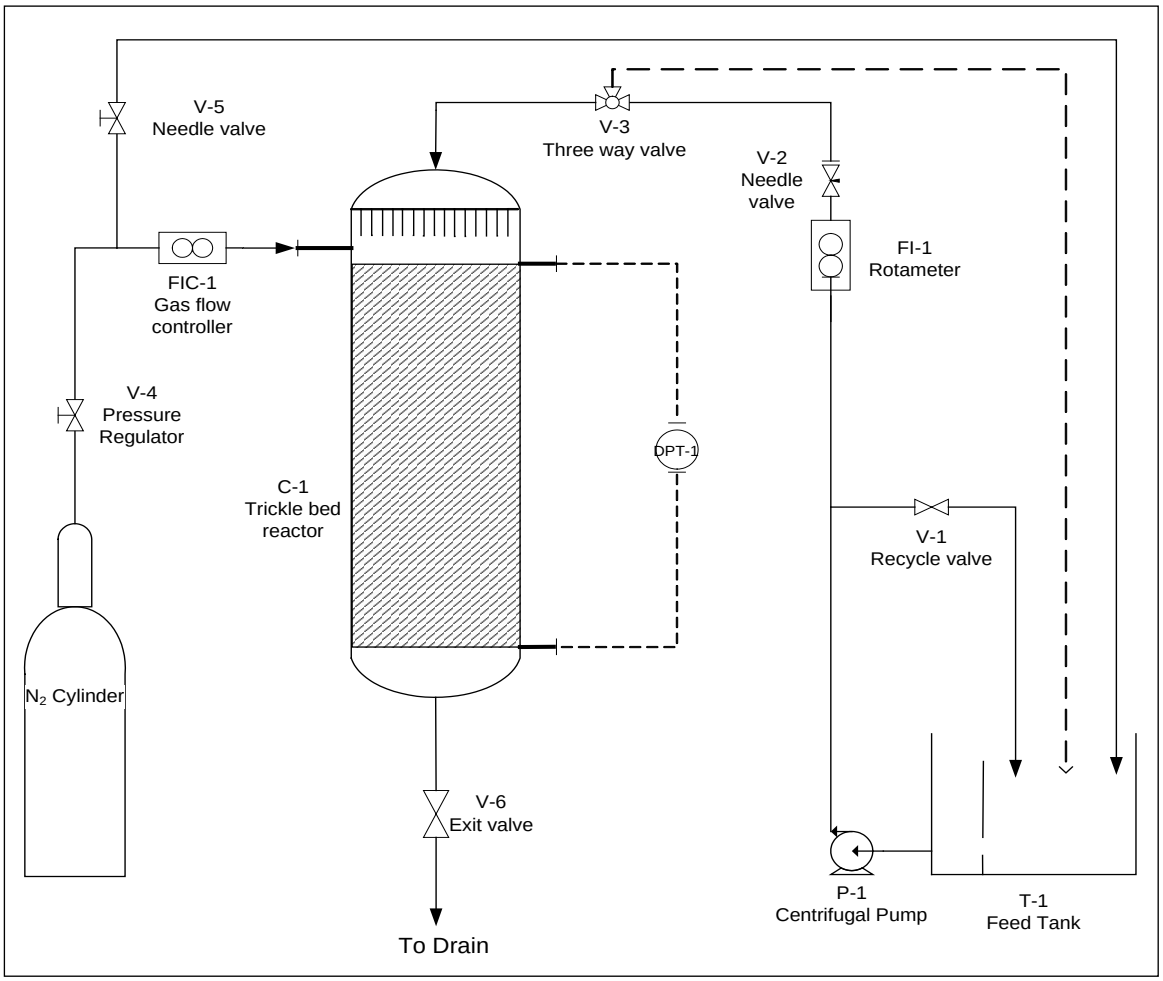

Figure 8: Flow diagram of experimental setup 1

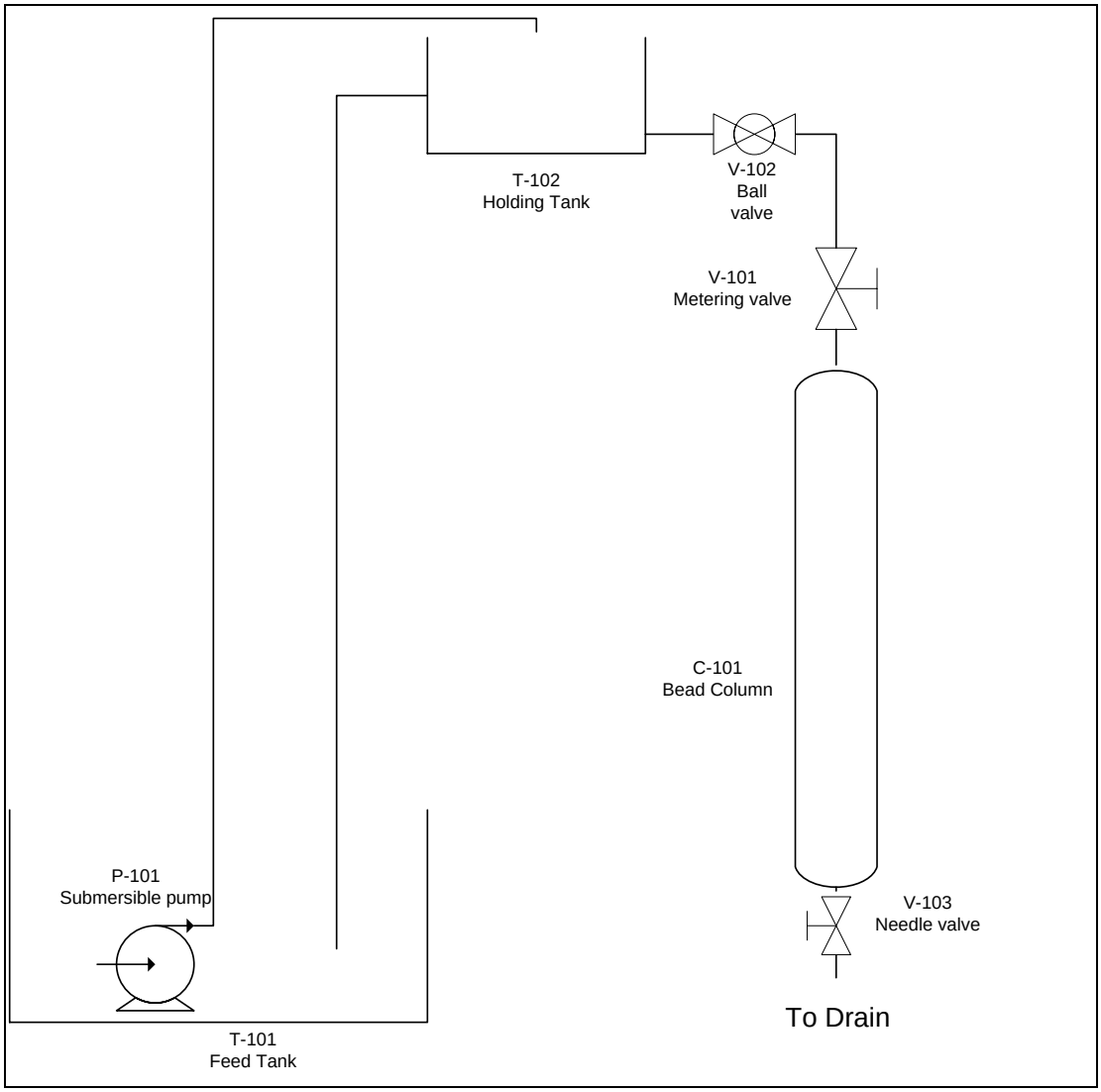

Figure 9: Flow diagram of experimental setup 2

The first setup, illustrated in figure 8, was used for the larger diameter columns employed in this study with internal diameters of 12, 20 and 40 mm. This setup comprised of a nitrogen gas system and liquid system which are fed concurrently to the top of each reactor. The second setup, represented in figure 9, was used for the bead column with an internal diameter of 5 mm and consisted of a liquid flow system. This liquid flow system was designed such that the liquid is pumped from a feed tank to a surge tank where the liquid flows under gravity to the bead column. The experiments were conducted at atmospheric temperature and pressure for comparison with data and correlations from previous studies.

The liquid feed systems for both setups have recycles as low liquid flow rates were required. The feed tank (T-1) for first setup has a weir to reduce the effect of turbulence from the recycle line and to ensure a constant pressure head. In the second setup, a submersible pump (P-101) was used to pump the liquid from the feed tank (T-101) to the surge tank (T-102) where an overflow pipe to the feed tank ensures a constant pressure head.

The gas flow rate was controlled by two Brooks Smart Mass flow controllers in order to encompass the gas flow rate range required. The 5850s model was used for the higher flow rate required in the 40mm column since it was calibrated to measure nitrogen in the range 0-20 l/min with an accuracy of 0.7% of the range. The Brooks 5851 model, which was calibrated to measure hydrogen in the range 0-30 l/min, was recalibrated to measure nitrogen in the range 0-2.2 l/min such that it could be employed for accurately controlling the lower gas flows. In order to prevent oxidation of the liquid by air, which is accelerated by the recycling of liquid, nitrogen was bubbled through the feed tanks in each setup.

The liquid flow rate for the first setup was measured by a set of 3 rotameter tubes (FI-1), which enabled flow rate measurement in the range of 1-1842 ml/min. The liquid flow was regulated using a gate valve (V-1) to control the bulk flow rate and a needle valve (V-2) at the exit of each rotameter tube to fine tune the flow to the column accurately. A three way valve (V-3) was used to recycle the liquid to the feed tank when the column was drained. The liquid flow to the bead column (C-101) in the second setup was controlled using a calibrated metering valve (V-101).

The liquid flow was fed to each column through needle type distributor plates in the first setup, as illustrated in figure 10. The needle type distributor was found provide superior liquid distribution than the perforated plate distributor employed by previous studies on trickle bed reactors (Loudon et al, 2006; Joubert & Nicol, 2009). The needles used were 40 mm long and had diameter of 1.2 mm. The distributor plates comprised of 7, 11 and 26 needles for the 12mm, 20mm and 40mm columns respectively to ensure uniform liquid distribution in each column. A nozzle was used to feed the liquid to the column in the second setup. The gas flow to the columns in

the first setup was fed through a side inlet 5 cm below the liquid distributor plate as it did not significantly impact the entry liquid distribution.

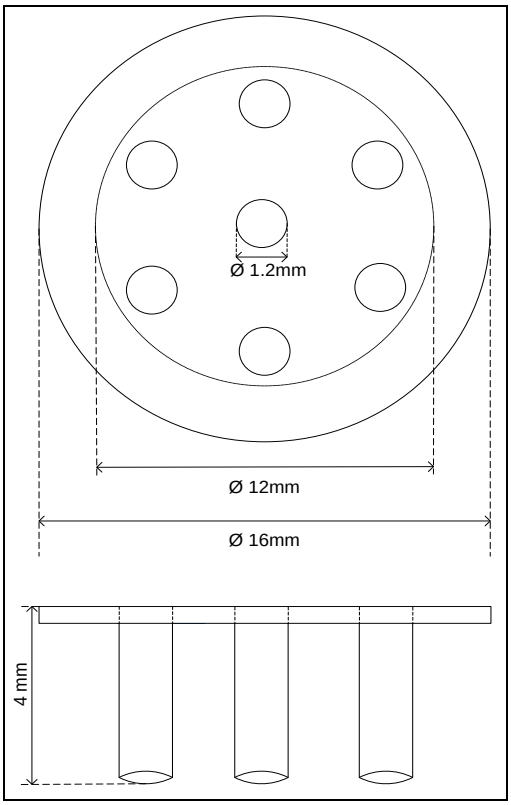

Figure 10: Distributor plate layout for the 12mm column

3.2. Operating procedure

3.2.1 Porosity

Each reactor consisted of a 1m long Plexiglass column packed with 4mm glass spheres up to a height of 0.91m. The columns were packed by pouring the beads in the column according to 'poured random packing' mode outlined by de Klerk (2006). A metal sieve was used to support the packing at the base of the column and to prevent the build up of liquid in the column. The amount of beads packed in each column was counted and the bed porosity calculated. The average porosities in the 12mm, 20mm and 40mm columns were 0.41, 0.40 and 0.38 respectively.

3.2.2 Liquid and gas flow rates

The liquid and gas flow rates were selected to cover most of the trickle flow regime in each of the columns and to enable comparison with literature data. The liquid superficial velocities employed in all the columns were 1, 2, 3, 4 and 5 mm/s. The highest value of liquid velocity was limited by the trickle-pulsing flow boundary in the 12mm column. Experiments with no gas flow were conducted for all the columns while experiments employing a gas velocity of 40mm/s were performed in the columns from the first setup.

3.2.3 Prewetting procedures

Prior to establishing the fluid flow rates at the operating flow rates, the packed beds were prewetted in order to investigate the effect of hydrodynamic multiplicity on the liquid solid mass transfer coefficient. Four prewetting procedures were conducted in each of the columns from the first setup, two with gas flow (Kan and Levec gas) and two without gas flow (Super and Levec). However, only two prewetting procedures could be performed in the 5mm column as there was no gas flow in the second setup. The prewetting procedures employed are described in detail below:

- **Kan Prewetting**

  The gas flow was introduced in the column at the operating velocity of 40mm/s. The liquid flow rate was increased gradually until pulsing was observed along the entire bed length. This pulsing regime was confirmed by pressure drop readings indicated by a Rosemount Model 3051CD Pressure Transmitter (DPT-1). The pulsing regime was maintained for 2 minutes in order to ensure the bed is thoroughly prewetted. Thereafter, the liquid flow rate was decreased to the desired operating point and the flow patterns were allowed to stabilise for 5 minutes before liquid solid mass transfer measurements are made.

- **Levec gas prewetting**

  For Levec gas prewetting, the gas flow was set at the operating velocity of 40 mm/s and the column was flooded at a low liquid velocity (<1mm/s) to ensure no air bubbles were trapped in the packed bed. The differential pressure

connections were removed to prevent the build up of gas in the column and the connection at the bottom of the column was sealed. Once the column was completely flooded, the liquid flow rate was recycled to the feed tank and the column was drained. The column was allowed to drain for 10 minutes to ensure only residual holdup liquid remained in the column. The differential pressure connections were then re-attached and the liquid was introduced at its operating velocity. Measurements were taken after 5 minutes to allow the flow patterns to become stable.

- **Levec prewetting**

This prewetting procedure was performed in the same manner as the Levec gas prewetting with the exception that there was no gas flow throughout the prewetting procedure and during operation.

- **Super prewetting**

The super prewetting procedure was also carried out without gas flow. The differential pressure connections are removed and the column is flooded at a low liquid flow rate (<1mm/s) to ensure no air bubbles are trapped in the packed bed. Once the packed section of the column was flooded, the liquid flow was adjusted to the desired operating flow rate and the column was subsequently drained. No gas flow was introduced during the operating procedure. Measurements were taken once a steady flow pattern was attained.

3.2.4 Liquid solid mass transfer experiments

The electrochemical technique is a popular experimental method employed by many studies for the accurate measurement of liquid solid mass transfer coefficients (Chou et al, 1979; Jolls & Hanratty, 1969, Latifi et al, 1997). This method is based on applying an electric potential to drive an electrochemical reaction which results in a flow of electrons and the resulting current is measured.

The electrochemical technique is effective in determining the liquid solid mass transfer coefficient since the measured current may be limited by either the mass transfer of the reactants to the surface of the electrode or the rate of electron transfer

associated with the kinetics of the electrochemical reaction. The range of applied voltage determines whether the rate of the reaction and consequently the limiting current is either mass transfer limited or kinetically limited. For liquid solid mass transfer coefficient measurements, the voltage applied to the cathode is controlled such that mass transfer rate of the reacting ions to the surface of the electrode limits the overall rate of the process rather than the kinetics of the redox reaction. This region is termed the *diffusion plateau* and indicates where the electrode is polarised since an increase in applied voltage yields the same current. The *diffusion plateau*, as illustrated in figure 11, was determined by Joubert (2009) using the same electrolyte and a single bead cathode at the same height in the packed bed as this study.

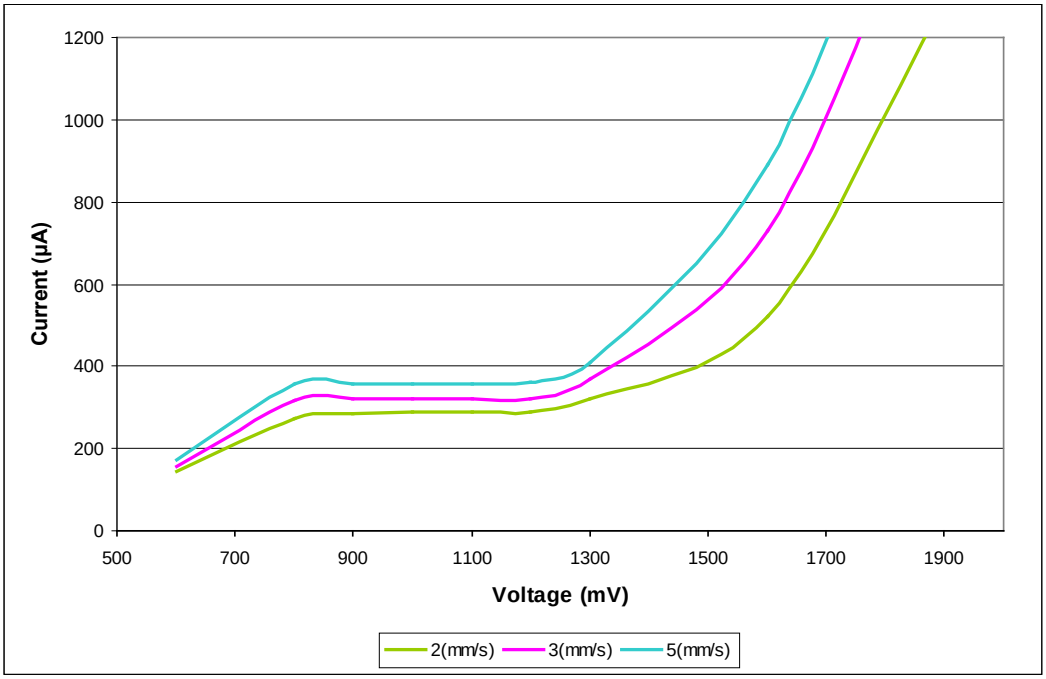

Figure 11: Diffusion plateau for electrode placement at a bed height of 65cm (Joubert, 2009)

The portion of the curve below the diffusion plateau indicates the region where the kinetics of the reduction reaction determines the rate of reaction at the electrode surface. Along the *diffusion plateau* region, the limiting current generated from the electrochemical process that takes place on the surface of the electrode (electrode – solution interface) is directly proportional to the liquid solid mass transfer coefficient according to the following relationship (Hanratty and Campbell, 1983).

$$I_{\lim} = n_e F k_{ls} A\, C$$

For the electrolyte system the concentration of ferricyanide is the same as the initial concentration and the remains n_e is equal to one for the ferricyanide reaction. The electrochemical method cannot measure the actual liquid solid mass transfer coefficient, k_{ls}, independently from the wetted solid area, A_e. Therefore, for partial wetting conditions an effective liquid solid mass transfer coefficient ($k_{ls}\phi$) is measured and A is replaced by ϕA, the active liquid-solid surface area. Therefore the effective liquid solid mass transfer coefficient is related to the instantaneous limiting current measured according to the following equation.

$$\phi k_{ls} = \frac{I_{\lim}}{n_e FCA}$$

The experimental setup used for the electrochemical measurement of the mass transfer coefficient is illustrated in Figure 12. A digital multimeter (NI PXI-4071 7 ½ Digit Flex DMM from National Instruments) was used to measure the limiting current. The mutimeter was connected in series to the electric circuit such that the cathode was attached to the negative pole of the voltage source and the anode was connected to the negative pole of the multimeter. The liquid solid mass transfer measurements were conducted at an applied voltage of 1V in order to ensure operation in the mass transfer limited regime. Following each prewetting procedure applied to each column, the measurements were taken at constant gas flow for each liquid flow rate which was increased from 1mm/s to 5mm/s. The limiting current measurements at each flow rate were taken at steady state, which was attained at approximately 7 minutes after applying a voltage across the electrodes.

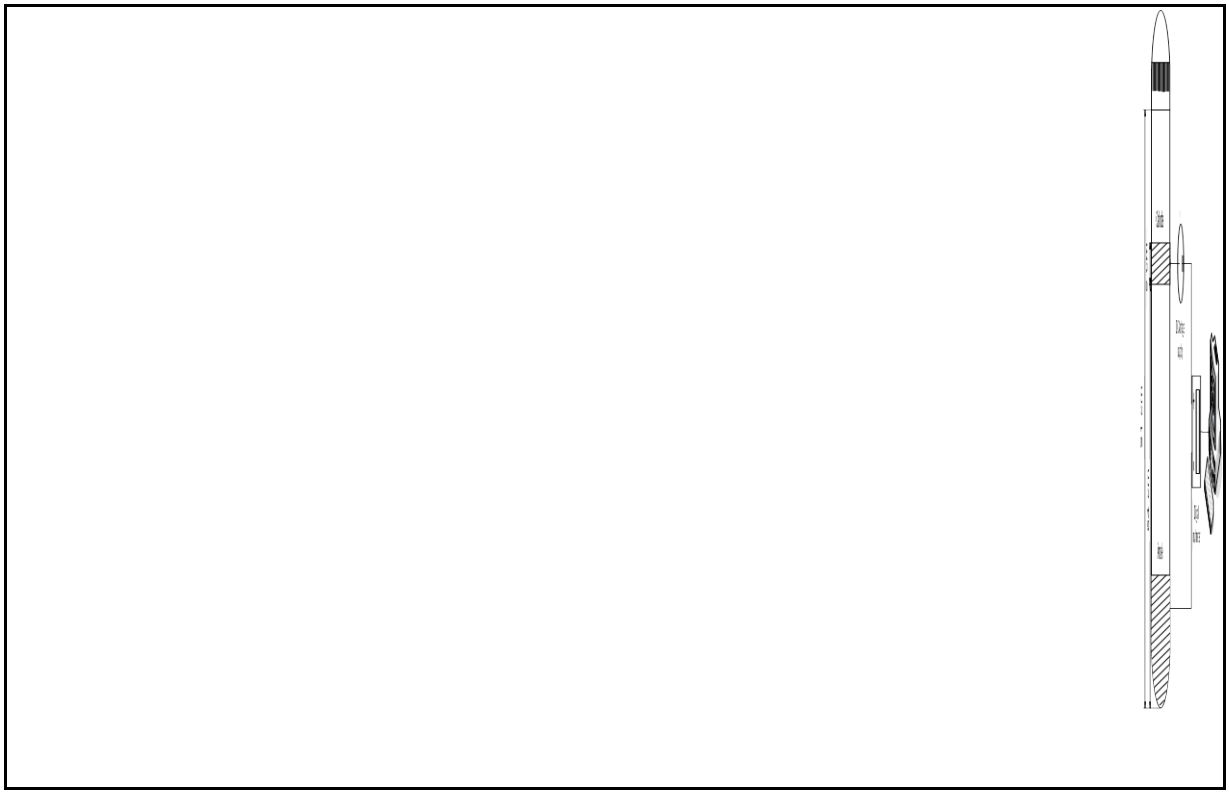

Figure 12: Experimental setup for the electrochemical technique

The chemical reaction at the electrode surfaces is initiated by the application of a negative voltage to the cathode. The electrodes employed were 4.5 mm nickel coated beads which replaced a 5 cm section of the packed bed for the cathode. The amount of beads used per electrode in each column is tabulated in Table 5 below. This type of electrode is referred to a multiple packing electrode and has been proven to be successful at providing accurate measurements of liquid solid mass transfer as it is not affected by radial dispersion (Delaunay et al, 1982, Joubert, 2009). The anode was positioned downstream of the cathode, at the exit of the bed and had a surface area twice that of the cathode to ensure that reduction at the cathode is the limiting reaction. The cathode was positioned at a height of 26 cm from the bed entrance such that it is not affected by entrance effects in the trickle flow regime.

The hexacyanoferrate redox system was chosen for the electrolyte since it has been successfully used in previous electrochemical studies on the liquid solid mass transfer coefficient (Delaunay et al, 1982, Jolls & Hanratty, 1969; Latifi et al, 1997; Chou et al, 1979). The electrolyte consisted of solution of 0.02M potassium

ferrocyanide ($K_4Fe(CN)_6$), 0.003M potassium ferricyanide ($K_3Fe(CN)_6$) and 1M of sodium hydroxide (*NaOH*) with distilled water as the solvent. The physiochemical properties of the electrolyte are listed in table 6.

Table 5: Number of beads per electrode in each column

Column inner diameter (mm)	Beads per cathode	Beads per anode
40	450	900
20	120	240
12	40	80
5	5	10

Table 6: Physiochemical properties of the electrolyte

Property	Value	Units
Density	1050	kg/m^3
Viscosity	$2.1x10^{-3}$	kg/m.s
Surface Tension	0.029	kg/s^2
Diffusion coefficient	$6.40x10^{-10}$	m^2/s

A large excess of sodium hydroxide was used to increase solution conductivity by reducing the electric field and subsequently minimising migration current (movement of ions along an electric field). This ensures that the transfer of reacting ions was only through molecular diffusion and convection effects. The concentration of the oxidising species was ten times higher than the reducing species in order to ensure that cathodic reduction is the limiting reaction. The redox reactions occurring at each electrode is illustrated below.

$$Fe(CN)_6^{3-} + e^- \rightarrow Fe(CN)_6^{4-} \qquad \text{(Cathode)}$$

$$Fe(CN)_6^{4-} \rightarrow Fe(CN)_6^{3-} + e^- \qquad \text{(Anode)}$$

Chapter 4 - Results and Discussion

4.1 Effect of column diameter on liquid solid mass transfer

Figure 13 illustrates the effective liquid solid mass transfer coefficients obtained from the different reactor sizes employed in the first setup (figure 5), at different liquid flow rates and for various prewetting procedures. Figure 14 is an alternative layout of the data in figure 13 to highlight the effect of gas on the liquid solid mass transfer coefficient. The measurement of the effective specific liquid solid mass transfer coefficient ($k_{ls}\phi$) reported in this study was based on the total geometric surface area rather than the actual wetted area since the external wetting efficiency could not be decoupled from the limiting current measurement.

On comparison with published correlations for the liquid solid mass transfer coefficients, the effective liquid solid mass transfer coefficients obtained in this study were two orders of magnitude lower. The precision of the results obtained was proven by repeating the measurements in all the columns for each prewetted mode, as illustrated in figure 14. An investigation into the accuracy of the measurement technique was also pursued in chapter 4.4. The relative variation for all the repeat runs was below 10%. Therefore, the data from this study was only used for qualitative purposes since the reason for the discrepancy of the results with published correlations could not be identified.

The effective specific liquid solid mass transfer coefficient showed a definite increase with a decrease in column diameter for all prewetting modes investigated in figure 13. The values for $k_{ls}\phi$ in the 12mm column were up to 3.3 times higher than the 40mm column and 1.9 times higher than the 20mm column. This result infers the possible influence of wall effects on the specific liquid solid mass transfer coefficient in reactors with low column to particle diameter ratios. These differences in $k_{ls}\phi$ values are most probably attributed to the variation of the liquid velocity profiles as

well as external wetted areas for the different column sizes. The reduction in column diameter resulted in an increase in average bed porosities which will reduce liquid holdup and subsequently increase liquid interstitial velocity in the packed bed. This is in agreement with the observed trend regarding the increase in liquid solid mass transfer as the column diameter is decreased. Although, Joubert (2009) showed that average interstitial velocities could not account for liquid solid mass transfer differences for the Kan and Levec gas prewetting modes. Therefore, the increase in interstitial velocity with a decrease in column diameter cannot justify a threefold increase in $k_{ls}\phi$. Furthermore, most liquid solid mass transfer correlations usually employ the square root of liquid velocity to account for the influence of liquid velocity which suggests that the liquid velocity impacts $k_{ls}\phi$ in a less than linear manner.

However, the external wetted area will affect $k_{ls}\phi$ linearly and as a result the significant differences in mass transfer are most probably caused by differences in external wetted area. Previous studies (Colombo et al, 1976; Van Houwelingen et al, 2006) on external wetting efficiency predict that the average external wetting in the largest column in this study (ID = 40mm), should approximately be in the region of 50% to 90%.Therefore, the increase in external wetted area upon decreasing the column to particle diameter ratio from 10 to 3 cannot substantiate a threefold increase in mass transfer.

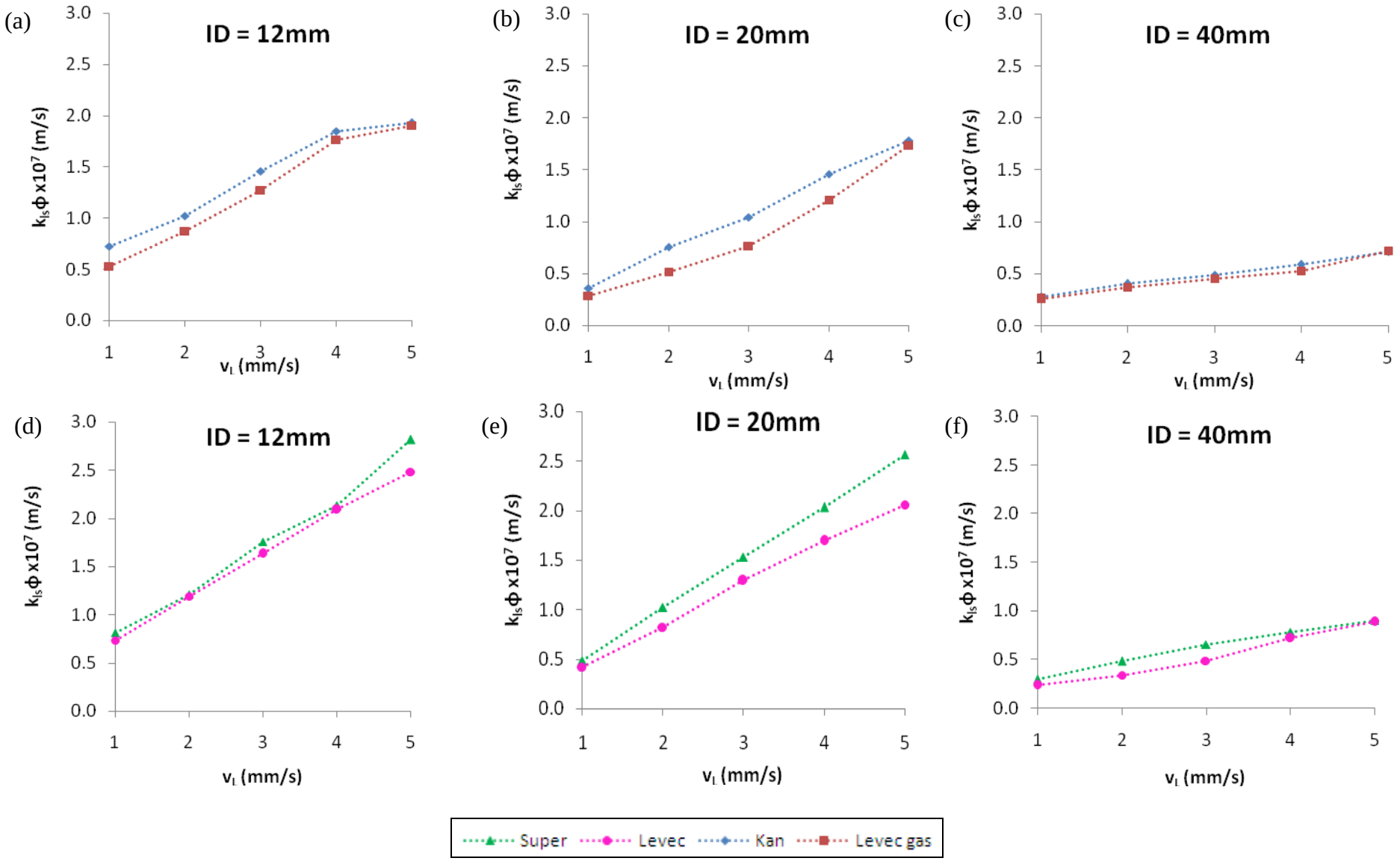

Figure 13: Effect of column diameter on the effective liquid solid mass transfer coefficient for the different prewetting modes

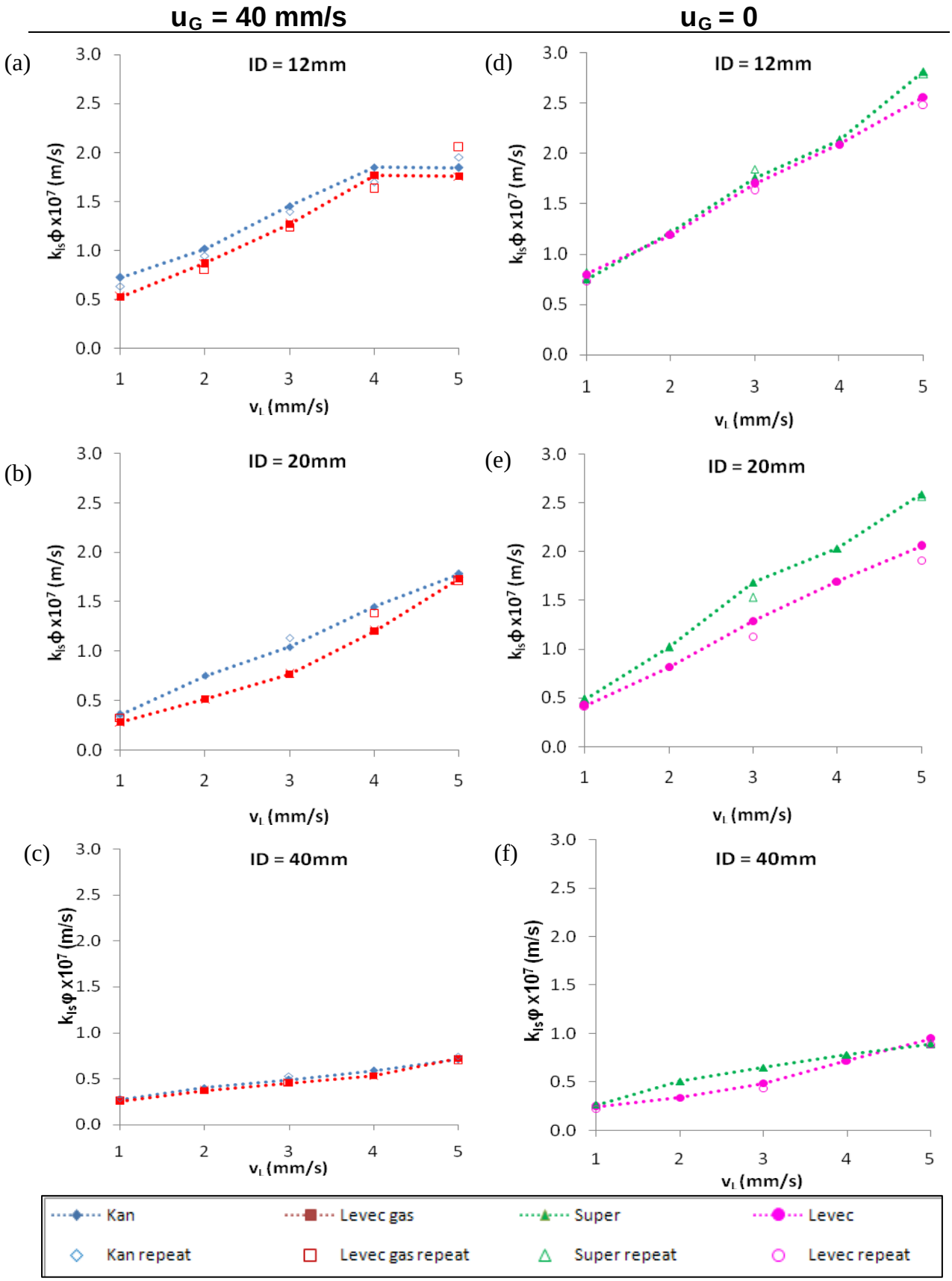

Figure 14: Effect of gas flow on the effective liquid solid mass transfer coefficient for different column diameters

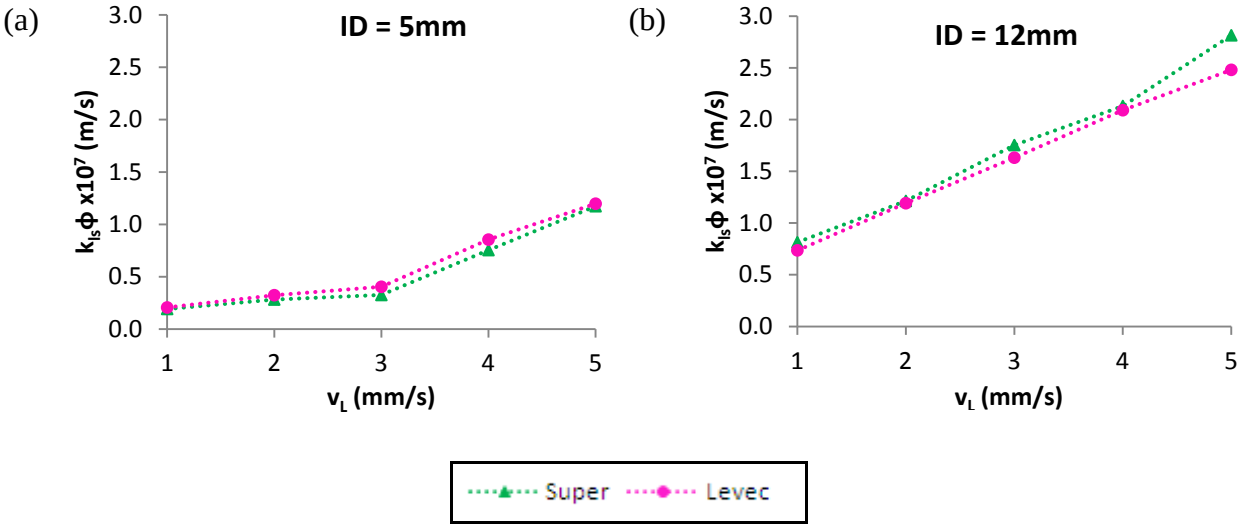

Figure 15: Effect of column diameter on effective liquid solid mass transfer for prewetting modes without gas flow

Figure 15 compares the liquid solid mass transfer results from the bead column (D/d_p =1) to the 12 mm column (D/d_p =3) for the super and Levec prewetting modes. The $k_{ls}\phi$ results from the 12 mm column were as much as 5 times higher than the bead column for low liquid flow rates (v_L<3mm/s) and 3 times higher for the higher liquid flow rates (v_L>3mm/s). This result goes against the trend of increasing effective liquid solid mass transfer with a reduction in column diameter and the reason for this behaviour could not be clearly defined. However, it was noted that the flow patterns in the bead column were drastically different compared to the columns in the first setup. At the low liquid flow rates (v_L<3mm/s) the liquid flowed as intermittent slugs through the column instead of a steady stream and as a result the electrode surface was not continuously wetted. The liquid flow pattern approached that of stream flow as the liquid superficial velocity was increased beyond 3 mm/s which caused the effective liquid solid mass transfer to increase sharply.

4.2 Hydrodynamic multiplicity effects on the liquid solid mass transfer coefficient

The effect of hydrodynamic multiplicity on the effective liquid solid mass transfer coefficient was investigated in all the columns by applying four prewetting procedures on the larger columns (D/d_p>1) namely Kan, Levec gas, Super and

Levec, as shown by figures 13 and 14. The latter two prewetting procedures as well their subsequent operation were conducted without gas flow in order to enable comparison with results from the bead column. The Super and Kan modes yielded higher mass transfer coefficients than the Levec and Levec gas modes respectively, in each of the columns as can be seen in figure 13. This can be attributed to the liquid film flow structures, associated with the Super and Kan prewetting procedures, which are more uniformly distributed in the bed cross section and result in a larger wetted area for liquid solid mass transfer. The appearance of distinct channels on the column walls for the Levec and Levec gas modes confirmed that non uniform rivulet flow is the predominant flow pattern in Levec prewetted packed beds. These trickle flow patterns for the different prewetting modes have also been confirmed by numerous studies on hydrodynamic multiplicity (Christensen et al, 1986; Lazzaroni et al, 1988; Lutran et al, 1991, Sederman & Gladden, 2001; van der Merwe & Nicol, 2005).

The hysteretic behaviour of the effective liquid solid mass transfer coefficient observed in Figures 13 (a), (b) and (c) indicates that Kan and Levec gas prewetting form the upper and lower boundaries for hydrodynamic multiplicity with gas flow for the columns in the first setup. The Kan mode yielded effective liquid solid mass transfer coefficients which were 1.4, 1.5 and 1.1 times higher than the Levec gas mode in the 12mm, 20mm and 40mm columns respectively. This trend was in agreement with the findings by Joubert & Nicol (2009) and Sims et al (1993). The increase in liquid solid mass transfer for Kan and Levec gas prewetting in the 12mm column between 4 mm/s and 5 mm/s was not as steep as the lower flow rates due to the inception of pulsing at 4mm/s.

The super prewetting mode yielded mass transfer coefficients that were 1.1, 1.3 and 1.2 times higher than the Levec mode in the 12, 20 and 40mm columns respectively. However, this trend was reversed in the bead column as the effective mass transfer coefficients from the Levec mode were as much as 1.2 times higher than the Super mode. This could be attributed to the low liquid renewal rate of stagnant pockets at low liquid superficial velocities (v_L<4mm/s) which, contrary to previous argument (Joubert & Nicol, 2009) appeared to be more prominent in the Super mode than Levec mode.

4.3 Effects of gas on Liquid Solid mass transfer coefficients

From figure 14 it is evident that the modes without gas flow outperformed the modes with gas flow. The effective liquid solid mass transfer coefficient values in the Levec prewetted mode were as much as 1.5, 1.7 and 1.3 times higher than values obtained for the Levec gas prewetted mode in the 12mm, 20mm and 40mm columns respectively. This is contrary to previous findings where gas flow was shown to have a minute influence on liquid solid mass transfer in the trickle flow regime (Delaunay et al, 1982; Satterfield et al, 1978). It also contradicts the proposals that gas flow enhances liquid solid mass transfer due to a reduction in the dynamic liquid holdup and the subsequent increase in the interstitial velocity of the liquid (Baussaron et al, 2007a; Trivizadakis & Karabelas, 2006c). In low column to particle diameter ratio columns, the channelling of liquid at the wall is significant. The gas flow in these columns enhances the wall effect rather than improving liquid distribution in the bed and instead causes more severe dry sections in the bed. This channelling behaviour was confirmed by the observation of distinct rivulets at the column wall especially for the Levec gas prewetted mode where the rivulets could be clearly identified at liquid superficial velocities up to 4 mm/s. Hence, the Levec gas prewetting mode yielded the lowest values for the effective liquid solid mass transfer coefficient in all the columns reported in figure 13.

4.4 Measurement technique validation

From section 4.1 it is evident that the low absolute readings and major variations of the liquid solid mass transfer coefficient across the various column diameters might be linked to the electrochemical measurement technique. Since this is a well established technique for liquid solid mass transfer measurement, no prior validation work was performed. However, this was deemed necessary following the results obtained for liquid solid mass transfer in the trickle flow regime for the various column diameters. Two possible reasons for the inaccurate measurements were

identified, namely the influence of nonfaradaic current on the limiting current measured and electrode inconsistencies.

The total limiting current measured across the electrodes in each reactor is the sum of two components namely, faradaic and nonfaradaic currents. The faradaic current is directly associated with the transfer of electrons from the reduction-oxidation reactions occurring at the electrodes while the nonfaradaic current is related to ohmic losses due to solution resistance of the neutral electrolyte component. It is necessary to determine the extent to which the nonfaradaic current affects the total limiting current and subsequently the effective liquid solid mass transfer coefficient. This effect will be more severe in the small diameter reactors due to the smaller electrode area available for the electrochemical reaction. Therefore, the nonfaradaic current was measured for a 1M sodium hydroxide solution for all prewetting modes in each of the columns from the first setup. This was done in order to ensure whether the increase in effective liquid solid mass transfer coefficient values with a decrease in column diameter was an accurate result free from resistance in the system. The percentage contribution of the nonfaradiac current to the total current measured, for all prewetting modes in each of the three column sizes at each liquid superficial velocity is reported in table 6. Unfortunately, the results were scattered over a wide range and showed no distinct trend with regard to an increase in superficial liquid velocity or column diameter, as observed for the total current measurements. Therefore, these results could not be applied with confidence to account for the nonfaradaic current contribution to the total limiting current measurements. Hence, the nonfaradaic current does not explain the significant liquid solid mass transfer differences.

Table 7: Nonfaradaic current percentages of the total current measured

COLUMN DIAMETER (mm)			**40**		
v_L (mm/s)	**1**	**2**	**3**	**4**	**5**
Kan	0.68	0.69	0.73	0.85	0.55
Levec Gas	0.75	0.40	0.88	0.77	0.74
Super	0.94	0.76	0.79	0.82	0.84
Levec	0.64	0.94	0.76	0.56	0.66
COLUMN DIAMETER (mm)			**20**		
v_L (mm/s)	**1**	**2**	**3**	**4**	**5**
Kan	0.79	0.90	0.49	0.80	0.77
Levec Gas	0.71	0.75	0.72	0.79	0.55
Super	0.74	0.82	0.46	0.71	0.54
Levec	0.81	0.84	0.63	0.80	0.58
COLUMN DIAMETER (mm)			**12**		
v_L (mm/s)	**1**	**2**	**3**	**4**	**5**
Kan	0.92	0.90	0.67	0.89	0.70
Levec Gas	0.69	0.89	0.81	0.68	0.93
Super	0.82	0.78	0.87	0.80	0.72
Levec	0.90	0.82	0.80	0.70	0.66

In order to further verify the trend of increasing effective liquid solid mass transfer coefficients with a decrease in column diameter, the specific liquid solid mass transfer coefficients, k_{ls}, were acquired for each column. This was obtained from flooding each reactor with liquid and then maintaining a constant liquid superficial velocity through the flooded bed. In this mode the electrode surfaces are completely wetted and the liquid solid mass transfer coefficient measured is free from the effects of liquid maldistribution and partial wetting. Hence, this single phase flow exhibits minimal wall effects and is therefore expected to yield column diameter independent liquid solid mass transfer measurements that ought to be comparable with published correlations.

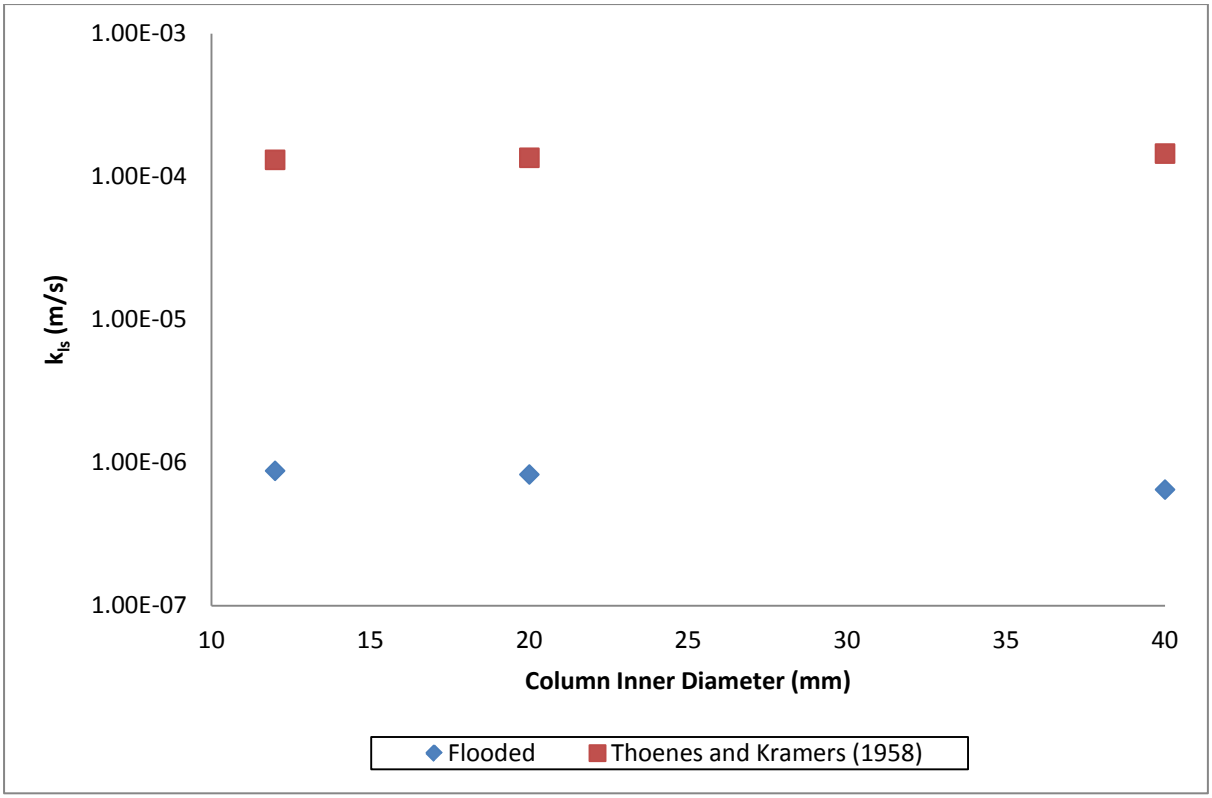

Figure 16: Comparison of specific liquid solid mass transfer coefficients with predicted values for single phase flow

A major deviation of the measured specific liquid solid mass transfer coefficients from the values predicted by the Thoenes and Kramers correlation (Fogler, 2006) as the column diameter decreased was apparent in figure 16. Unfortunately, the measurement technique validation efforts could not explain the low liquid solid mass transfer readings obtained in this study.

Chapter 6 – Conclusions and Recommendations

Conclusions

The effective liquid solid mass transfer coefficients obtained in this study were two orders of magnitude lower than published correlations therefore the results can only be used for comparison purposes. A general trend of an increase in effective liquid solid mass transfer with a decrease in column diameter was observed for the 12, 20 and 40mm columns. However, this trend was not sustained in the bead column which had the lowest effective liquid solid mass transfer coefficient values due to unsteady liquid flow patterns. A threefold increase in the effective liquid solid mass transfer coefficient was observed upon decreasing the column to particle diameter ratio from 10 to 3. However, this significant increase could not be completely validated by either external wetted area or interstitial velocity variations.

The effective liquid solid mass transfer coefficients in each column exhibited significant hydrodynamic multiplicity behaviour. The Kan mode yielded mass transfer coefficients that were 1.4, 1.5 and 1.1 times higher than the Levec gas mode in the 12mm, 20mm and 40mm columns respectively. This trend was in agreement with the findings by Joubert & Nicol (2009) and Sims et al (1993). The super mode rendered mass transfer coefficients that were 1.1, 1.3 and 1.2 times higher than the Levec mode in the 12, 20 and 40mm columns respectively.

The modes without gas flow outperformed the prewetting modes with gas flow. This was illustrated by the effective liquid solid mass transfer coefficient values obtained in the Levec prewetted mode which were as much as 1.5, 1.7 and 1.3 times higher in the Levec gas prewetted mode for the 12mm, 20mm and 40mm columns respectively. This result was attributed to the enhancement of the wall effects by the gas flow and the resulting severe dry sections in the bed reduce the wetted area for liquid solid mass transfer.

In an attempt to substantiate the threefold increase in mass transfer on decreasing the column to particle diameter ratio from ten to three, the measurement technique required validation. The electrochemical technique has been renowned for yielding reliable and accurate liquid solid mass transfer measurements. However, in this study the method could not account for low mass transfer coefficient values across the range of column diameters. The influence of nonfaradaic current on the total limiting current measured could not be identified due to the wide variation of the results.

Recommendations

This study provides scope for further investigation due to the lack of hydrodynamic parameter data in columns with low column to particle diameter ratios. Possible avenues of interest are:

The discrepancy in the true mass transfer coefficients in the flooded bed should be investigated to provide insight into the resistances present in the small diameter columns.

Accurate wetting efficiency data should be obtained to determine the true liquid solid mass transfer coefficients and to further validate the wall effects on liquid solid mass transfer in small diameter columns.

References

Al-Dahhan, M. H., Dudukovic, M. P., (1994) “Pressure drop and liquid holdup in high pressure trickle-bed reactors” *Chemical Engineering Science*, 49, 5681-5698

Al-Dahhan, M. H., Dudukovic, M. P., (1995) “Catalyst wetting efficiency in trickle-bed reactors at high pressure” *Chemical Engineering Science*, 50, 2377-2389

Attou, A., Boyer, C., Ferschneider, G., (1999) “Modelling of the hydrodynamics of the concurrent gas-liquid trickle flow through a trickle-bed reactor” *Chemical Engineering Science*, 54, 785-802

Baker, T., Chilton, T. H., Vernon, H.C., (1935) “The course of liquor flow in packed towers” *Trans. Am. Inst. Chem. Eng.*, 31, 296-313

Bartelmus, G., (1989) “Local solid-liquid mass transfer coefficients in a three-phase fixed bed reactor” *Chem. Eng. Process*, 26, 111-120

Baussaron, L., Julcour-Lebigue, C., Boyer, C., Wilhelm, A., Delmas, H., (2007a) “Effect of partial wetting on liquid/solid mass transfer in trickle bed reactors” *AIChE Journal*, 53, 1850-1860

Baussaron, L., Julcour-Lebigue, C., Boyer, C., Wilhelm, A., Delmas, H., (2007c) “Partial wetting on in trickle bed reactors: Measurement techniques and global wetting efficiency” *Ind. Eng. Chem. Res*., 46, 8397-8405

Benyahia, F., O’Neill, K. E., (2005) “Enhanced Voidage Correlations for packed beds of Various Particle Shapes and Sizes” *Particulate Science and Technology*, 23, 169-177

Butt, J. B., Weekman Jr, V. W., (1974) “Characterization of the activity, selectivity and aging properties of heterogeneous catalysts” *AIChE Symp. Ser*., 70, 27

Christensen, G., McGovern, S. J., Sundaresan, S., (1986) “Cocurrent Downflow of Air and Water in a Two-dimensional packed column” *AIChE Journal*, 32, 1677-1689

Chou, T. S., Worley, F. L., Luss, D., (1979) ”Local particle-liquid mass transfer fluctuations in mixed-phase concurrent downflow through a fixed bed in the pulsing regime” *Ind. Eng. Chem. Fundam*., 18, 279-283

Colombo, A. J., Baldi, G., Sicardi, S., (1976) “Solid-liquid contacting effectiveness in trickle bed reactors” *Chemical Engineering Science*, 31, 1101-1108

De Klerk, A., (2003) “Voidage variation in packed beds at small column to particle diameter ratio” *AIChE Journal*, 49, 2022-2029

Delaunay, C. B., Storck, A., Laurent, A., Charpentier, J. C., (1982) “Electrochemical determination of liquid-solid mass transfer in a fixed-bed irrigated gas-liquid reactor with downward concurrent flow” *Int. Chem. Eng*., 22, 244-251

Dudukovic, M. P., (1977) “Catalyst effectiveness factor and contacting efficiency in trickle-bed reactors” *AIChE Journal*, 23, 940-944

Fogler, H. S., “Elements of Chemical Reaction Engineering” Fourth Edition, Prentice Hall, (2006), 784

Fahien, R. W., Stankovic, I. M., (1979) “An equation for the velocity profile in packed columns” Chemical Engineering Science, 34, 1350-1354

Gabitto, J. F., Lemcoff, N. O., (1987) “Local solid-liquid mass transfer coefficients in a trickle bed reactor” The Chemical Engineering Journal, 35, 69-74

Gianetto, A., Specchia, V., (1992) “Trickle-bed reactors: state of art and perspectives” *Chemical Engineering Science*, 47, 3197-3213

Gierman, H., (1988), “Design of Laboratory Hydrotreating Reactors Scaling Down of Trickle-flow reactors” *Applied Catalysis*, 43, 277-286

Govindaro, V. M. H., Froment, G. F., (1986) “Voidage Profiles in packed beds of spheres” *Chemical Engineering Science*, 41, 533-539

Hanratty, T.J., Campbell, J. A., “Measurement of wall stress” in Goldstein, R. J., (1983) *Fluid Mechanics Measurements*, Hemisphere Publishing Corporation

Herskowitz, M., Smith, J. M., (1978) “Liquiddistribution in trickle-bed reactors: PartI. Flow measurements” *AIChE Journal*, 24, 439-450

Hoftyzer, P. J., (1964) “Liquid distribution in a column with dumped packing” *Trans. Instn. Chem. Eng*., 42, T109-T117

Holub, R. A., Dudukovic, M. P., Ramachandran, P. A., (1993) “Pressure drop, Liquid holdup and flow regime transition in trickle flow” *AIChE Journal*, 39, 302-321

Jolls, K. R., Hanratty, T. J., (1969) “Use of electrochemical techniques to study mass transfer rates and local skin friction to a sphere in a dumped bed” *AIChE Journal*, 15, 199-205

Joubert, R., (2009) “Solid liquid mass transfer in trickle bed reactors” Masters dissertation, University of Pretoria

Joubert, R., Nicol, W., (2009) “Multiplicity behaviour of trickle flow liquid-solid mass transfer” *Ind. Eng. Chem. Res*., 48, 8387-8392

Julcour-Lebigue, C., Augie, F., Maffer, H., Wilhelm, A., Delmas, H., (2009) “Measurements and modelling of wetting efficiency in trickle-bed reactors: Liquid viscosity and bed packing effects” *Ind. Eng. Chem. Res*., 48, 6811-6819

Kan, K.M., Greenfield, P.F., (1978) “Multiple hydrodynamic states in concurrent two-phase down-flow through packed beds” *Ind. Eng. Chem. Process. Des. Develop.*, 17, 482–485.

Kundu, A., Saroha, A. K., Nigam, K. D. P., (2001) “Liquid distribution studies in trickle-bed reactors” *Chemical Engineering Science*, 56, 5963-5967

Lakota, A., Levec, J., (1990) “Solid-liquid mass transfer in packed beds with concurrent downward two-phase flow” *AIChE Journal*, 36, 1444-1448

Larachi, F., Belfares, L., Iliuta, I., Grandjean, B. P. A., (2003) “Heat and Mass Transfer in cocurrent gas-liquid packed beds. Analysis, Recommendations, and new correlations” *Ind. Eng. Chem. Res.*, 42, 222-242

Larachi, F., Belfares, L., Grandjean, B. P. A., (2001) “Prediction of liquid-solid wetting efficiency in trickle flow reactors” *Int. Comm. Heat Mass Transfer*, 28, 595-603

Larachi, F., Laurent, A., Midoux, N., Wild, G., (1991) “Experimental study of a trickle bed reactor operating at high pressure: two-phase pressure drop and liquid saturation” *Chem. Eng. Sci*., 46, 1233-1246

Latifi, M. A., Naderifar, A., Midoux, N., (1997) “Experimental investigation of the liquid/solid mass transfer at the wall of a trickle-bed reactor-influence of Schmidt number” *Chemical Engineering Science*, 52, 4005-4011

Latifi, M. A., Laurent, A., Wild, G., Storck, A. (1994) “Wall-to-liquid mass transfer in a packed-bed reactor: influence of Schmidt number” *Chemical Engineering and Processing*, 33, 189-192

Lazzaroni, C. L., Keselman, H. R., Figoli, N.S., (1988) “Colorimetric evaluation of the efficiency of liquid-solid contacting in trickle flow” *Ind. Eng. Chem. Res*., 27, 1132-1135

Levec, J., Saez, A. E., Carbonell, R. G., (1986) “The hydrodynamics of trickling flow in packed beds Part II: Experimental Observations” *AIChE Journal*, 32, 369-380

Llano, J. J., Rosal, R., Sastre, H., Diez, F. V., (1997) “Determination of wetting efficiency in trickle-bed reactors by a reaction method” *Ind. Eng. Chem. Res*., 36, 2616-2625

Loudon, D., Van der Merwe, W., Nicol, W., (2006) “Multiple hydrodynamic states in trickle flow: Quantifying the extent of pressure drop, liquid holdup and gas-liquid mass transfer variation” *Chemical Engineering Science,* 26, 7551-7562

Lutran, P. G., Ng, K. M., Delikat, E. P., (1991) “Liquid distribution in trickle beds: An experimental study using computer-assisted tomography” *Ind. Eng. Chem. Res*., 30, 1270-1280

Maiti, R., Khanna, R., Nigam, K. D. P., (2006) “Hysteresis in trickle-bed reactors: A review” *Ind. Eng. Chem. Res.,* 45, 5185-5198

Marivoet, J., Teodoroiu, P., Wajc, S. J., (1974) “Porosity, velocity and temperature profiles in cylindrical packed beds” *Chem. Eng. Sci*., 29, 1836-1840

Mears, D. E.,(1971) “Tests for transport limitations in experimental catalytic reactors” *Ind. Eng. Chem. Process. Des. Develop*, 10, 541-547

Mederos, F. S., Ancheyta, J., Chen, J., (2009) “Review on criteria to ensure ideal behaviours in trickle-bed reactors” *Applied Catalysis A: General*, 355, 1-19

Mueller, G. E., (1991) “Prediction of radial porosity distributions in randomly packed fixed beds of uniformly sized spheres in cylindrical containers” *Chem. Eng. Sci*., 46, 706-708

Niu, M., Akiyama, T., Takahashi, R., Yagi, J., (1996) “Reduction of the wall effect in a packed bed by a hemispherical lining” *AIChE Journal,* 42, 1181-1186

Onda, K., Takeuchi, H., Maeda, Y., Takechi, N., (1973) “Liquid distribution in a packed column” *Chemical Engineering Science,* 28, 1677-1683

Patwardhan, V. S., Pataskar, S. G.,(1982) “The influence of wettability on the equilibrium wall flow of liquid in a packed column” *The Chemical Engineering Journal*, 23, 145-149

Perego, C., Peratello, S., (1999) “Experimental methods in catalytic kinetics” *Catalysis Today*, 52, 133-145

Pironti, F., Mizrahi, D., Acosta, A., Gonzalez-Mendizabal, D., (1999) “Liquid-solid wetting factor in trickle-bed reactors: its determination by a physical method” *Chemical Engineering Science*, 54, 3793-3800

Ridgway, K., Tarbuck, K. J., (1968) “Voidage fluctuations in randomly-packed beds of spheres adjacent to a containing wall” *Chem. Eng. Sci*., 23, 1147-1155

Saroha, A. K., Nigam, K. D. P., Saxena, A. K., Kapoor, V. K., (1998) “Liquid Distribution in trickle-bed reactors” *AIChE Journal*, 44, 2044-2052

Satterfield, C. N., Van Eek, M. W., Bliss, G. S., (1978)“ Liquid-Solid Mass Transfer in packed beds with downward concurrent gas-liquid flow” *AIChE Journal*, 24, 709-717

Satterfield, C. N., (1975) “Trickle bed reactors” *AIChE Journal*, 21, 209-228

Sederman, A. J., Gladden, L. F., (2001) “Magnetic resonance imaging as a quantative probe of gas-liquid distribution and wetting efficiency in trickle bed reactors” *Chemical Engineering Science*, 56, 2615-2628

Sicardi, S., Baldi, G., Gianetto, A., Specchia, V., (1980) “Catalyst areas wetted by flowing and semistagnant liquid in trickle-bed reactors” *Chemical Engineering Science*, 35, 67-73

Sie, S.T., Krishna, R., (1998) “Process Development and Scale up: III. Scale-up and scale-down of trickle bed processes” *Reviews in Chemical Engineering*, 14, 203-252

Sims, W., Schultz, F. G., Luss, D., (1993) “Solid-Liquid mass transfer to hollow pellets in a trickle bed” *Ind. Chem. Eng. Res*., 32, 1895-1903

Specchia, V., Baldi, G., Gianetto, A., (1978) “Solid-liquid mass transfer in concurrent two-phase flow through packed beds” *Ind. Eng. Chem. Process Des. Dev*., 17, 362-367

Templeman, J. J., Porter, K. E., (1965) “Experimental determination of wall flow in packed columns” *Chemical Engineering Science*, 20, 1139-1140

Trivizadakis, M. E., Karabelas, A. J., Giakoumakis, D., (2006a), “A study of particle shape and size effects on hydrodynamic parameters of trickle beds” *Chemical Engineering Science*, 61, 5534-5543

Trivizadakis, M. E., Karabelas, A. J., (2006c), “A study of local liquid/solid mass transfer in packed beds under trickling and induced pulsing flow” *Chemical Engineering Science*, 61, 7684-7696

Van der Merwe, W., (2008), “Trickle flow hydrodynamic multiplicity” PhD thesis, University of Pretoria

Van der Merwe, W., Nicol, W., (2005) “Characterization of multiple flow morphologies within the trickle flow regime” *Ind. Eng. Chem. Res*., 44, 9446-9450

Van der Merwe, W., Nicol, W., (2009) “Trickle flow hydrodynamic multiplicity: Experimental observations and pore-scale capillary mechanism” *Chem. Eng. Sci*., 64, 1267-1284

Van Houwelingen, A., Sandrock, C., Nicol, W., (2006) “Particle wetting distribution in trickle-bed reactors” *Chem. Eng. Sci*., 62, 5543-5548

Van Houwelingen, A., Van der Merwe, W., Nicol, W., (2007) “Extension of liquid-limited trickle-bed reactor modelling to incorporate channelling effects” *AIChE Jounal*, 52, 3532-3542

Van Houwelingen, A., Nicol, W., (2010) “Parallel hydrogenation for the quantification of wetting efficiency and liquid solid mass transfer” *AIChE*, DOI: 10.1002/aic.12342

Van Houwelingen, A., (2006), “The morphology of solid liquid contacting efficiency in trickle flow” Masters dissertation, University of Pretoria

Wang, J., “Analytical Electrochemistry”, Third edition, John Wiley & Sons, Inc., (2006), Pages 1-28

Zoski, C. J., “Handbook of Electrochemistry”, First edition, Elsevier B. V., (2007), Pages 1-28